Applications and Research Using Remote Sensing for Rangeland Management

E. Raymond Hunt, Jr., James H. Everitt, Jerry C. Ritchie, M. Susan Moran, D. Terrance Booth, Gerald L. Anderson, Patrick E. Clark, and Mark S. Seyfried

Abstract

Rangelands are grasslands, shrublands, and savannas used by wildlife for habitat and livestock in order to produce food and fiber. Assessment and monitoring of rangelands are currently based on comparing the plant species present in relation to an expected successional end-state defined by the ecological site. In the future, assessment and monitoring may be based on indicators of ecosystem health, including sustainability of soil, sustainability of plant production, and presence of invasive weed species. USDA Agricultural Research Service (ARS) scientists are actively engaged in developing quantitative, repeatable, and low-cost methods to measure indicators of ecosystem health using remote sensing. Noxious weed infestations can be determined by careful selection of the spatial resolution, spectral bands, and timing of image acquisition. Rangeland productivity can be estimated with either Landsat or Advanced Very High Resolution Radiometer data using models of gross primary production based on radiation use efficiency. Lidar measurements are useful for canopy structure and soil roughness, indicating susceptibility to erosion. The value of remote sensing for rangeland management depends in part on combining the imagery with other spatial data within geographic information systems. Finally, ARS scientists are developing the knowledge on which future rangeland assessment and monitoring tools will be developed.

Introduction

Rangelands are a type of land resource, which is characterized by non-forest, native vegetation (NRCS, 1997). Landcover types of rangelands are grasslands, shrublands, and savannas, which are determined by climate. Generally, large year-to-year variability of precipitation make rangelands unsuitable for crop production, and livestock grazing presents a sustainable means of food and fiber production. Drought conditions, which often last years, may drastically affect plant community composition and may make rangelands more susceptible to diseases, insect pests, weed invasions, and overgrazing. Healthy rangelands are a national resource that will sustain soil quality, enhance the availability of clean water, sequester excess carbon dioxide, maintain plant and animal diversity, and support a myriad of other non-agricultural uses (Follett *et al.*, 2001).

The extent of rangelands is large, both for the United States and for the world. Different authors use different criteria for determining these areas. The Natural Resources Inventory (NRCS, 1994) estimates the extent of privately owned rangeland in the United States to be 1.62×10^6 km^2 for about 21 percent of the total area. Using Landsat Thematic Mapper data, Vogelmann *et al.* (2001) determined that shrublands and grasslands are 34 percent of the total area in the conterminous USA. Monitoring such large areas at low cost is the forte of remote sensing.

So why isn't remote sensing currently applied for rangeland management? Since the beginning of remote sensing as a discipline, scientists have been studying potential applications (Tueller, 1982; Carneggie *et al.*, 1983; Tueller, 1989; Tueller, 1992; Tueller, 1995). As discussed in the next section, there is a mismatch between the information wanted by range managers and the information provided by remote sensing. This situation is changing; a report by the National Research Council suggests that criteria for management should be related to ecosystem health (NRC, 1994). With the recent availability of a wide variety of sensors and platforms, there is considerable research in remote sensing that is being applied to rangelands. It is the purpose of this review to show how USDA-ARS research in the field of remote sensing can be used to provide important information related to ecosystem health for monitoring rangelands.

Rangeland Management and the Potential of Remote Sensing

At the beginning of the 20th Century, studies on plant succession, the gradual, progressive change of community types from initial colonizers to climax vegetation, formed one of the theoretical bases of plant ecology as a scientific discipline (Clements, 1916; Sampson, 1919). The climax plant community, determined by climate, was supposed to have the highest sustainable productivity, to be the most resistant to weed establishment, and to provide the best protection against soil erosion. Overgrazing reverses the direction of plant succession from climax to earlier successional stages (Sampson, 1919).

The first practical methodology for rangeland monitoring was developed by Dyksterhuis (1949). Basically, the weight or cover of each species in a plot was determined

E.R. Hunt, Jr., and J.C. Ritchie are with the Hydrology and Remote Sensing Laboratory, USDA Agricultural Research Service, Building 007, Room 104, 10300 Baltimore Ave., Beltsville, MD 20705 (erhunt@hydrolab.arsusda.gov).

J.H. Everitt is with the Kika de la Garza Subtropical Agricultural Research Center, USDA Agricultural Research Service, 2413 E. Highway 83, Weslaco, TX 78596.

M.S. Moran is with the Southwest Watershed Research Center, USDA Agricultural Research Service, 2000 E. Allen Rd., Tucson, AZ 85719.

D.T. Booth is with the High Plains Grasslands Research Station, USDA Agricultural Research Service, 8408 Hildreth Rd., Cheyenne, WY 82009.

G.L. Anderson is with the Northern Plains Agricultural Research Laboratory, USDA Agricultural Research Service, 1500 North Central Ave., Sidney, MT 59270.

P.E. Clark and M.S. Seyfried are with the Northwest Watershed Research Center, USDA Agricultural Research Service, 800 Park Blvd., Suite 105, Boise, ID 83712.

Photogrammetric Engineering & Remote Sensing
Vol. 69, No. 6, June 2003, pp. 675–693.

0099-1112/03/6906–675$3.00/0

and classified as climax species or not. Range "condition" is calculated from the percent climax vegetation present: 76 to 100 percent climax vegetation is excellent, 51 to 75 percent is good, 26 to 50 percent is fair, and 0 to 25 percent is poor. This method, with minor modifications, was used by the Natural Resource Conservation Service (NRCS) for private grazing lands, and by the Bureau of Land Management (BLM) and the Forest Service (FS) for federally owned grazing lands.

The current theory on succession for range management has changed from a single climax community to multiple end-state communities with "State and Transition Models" (Friedel, 1991; Laycock, 1991). Furthermore, each part of the landscape is no longer compared to the same climax; "ecological sites," which are defined by different potentials for plant production, are delineated on the basis of soils, topography, hydrology, and other factors (SRM, 1995). Whereas the NRCS and other agencies consider the assessment of rangeland health to be important and are working on a rating system, the methodology of comparing the species present with the presumed successional end-state for a given ecological site (termed a similarity index) is the current basis of rangeland assessment (NRCS, 1997).

Therefore, many rangeland managers want some method using remote sensing that would classify an area based on the successional status of the species present, not a general land-cover classification. Interpretation of large-scale aerial photography allows many species to be identified by the patterns and shapes of the plant clumps and crowns, but computer algorithms do not yet have the ability to recognize the different complex patterns. Digital image processing of satellite data, even with small pixel sizes, can determine land cover but not individual plant species. The reflectance spectrum from remotely sensed vegetation contains information on the chlorophyll content, water content, and leaf and canopy structure (Gates *et al.*, 1965; Knipling, 1970). There is no spectral signature for successional status, and it is unlikely that satellite data will ever provide managers with rangeland "condition," or other indices based on plant succession.

Another basis for assessment is rangeland ecosystem health, which is defined "as the degree to which the integrity of the soil and the ecological processes of rangeland ecosystems are sustained" (NRC, 1994). The amount and type of soil erosion are one set of indicators on the degree of rangeland health; the amount of plant production and plant residue are other indicators of a healthy ecosystem (Pellant *et al.*, 2000). More recently, there is an awareness that presence of noxious invasive species may be an indicator of poor ecosystem health (Vitousek *et al.*, 1996; Sheley and Petroff, 1999, Pellant *et al.*, 2000). There are valid concerns about how the various potential indicators are quantified and weighted into an overall estimate of ecosystem health (West and Smith, 1997). In a comparison of 149 inventory points in western Colorado, Spaeth *et al.* (1999) found no significant correlation between similarity index and 17 different indicators of rangeland health. However, the costs for this survey suggest that assessment for ecosystem health, on the ground, for one randomly selected location, would be about $500 (Pellant *et al.*, 1999), so a statistically accurate rangeland survey for the United States would cost on the order of ten million dollars.

The challenge remains to define cost-effective indicators and methods for rangeland assessment and monitoring. Remote sensing can provide direct estimates for many of the indicators proposed for ecosystem health at lower cost. USDA-ARS scientists involved with remote sensing are actively conducting research using proven and new technologies, capable of monitoring key indicators of ecosystem health, over the vast extent of rangelands.

Remote Sensing of Noxious Rangeland Plant Species

Noxious brush and weeds dominate the vegetation of many rangeland plant communities and frequently pose the primary deterrent to effective management of these areas (Scifres, 1980). Rangeland areas are generally extensive and inaccessible; consequently, determining the distribution and extent of infestations or botanical characteristics by ground surveys is difficult. More accurate measurements of area infested and canopy cover are essential to estimating the amount of damage or ecological impact caused by invading brush and weeds. Remote sensing techniques offer rapid acquisition of data with generally short turnaround time at costs lower than ground surveys (Tueller, 1982; Everitt *et al.*, 1992).

The value of remote sensing for distinguishing some plant species and communities on rangelands is well established (Carneggie *et al.*, 1983; Tueller, 1989; Everitt *et al.*, 1995; Driscoll *et al.*, 1997; Everitt *et al.*, 2001a). Field reflectance measurements have been used to distinguish noxious plant species (Gausman *et al.*, 1977a; Everitt *et al.*, 1987; Lass and Callihan, 1997). Likewise, aerial photography, airborne videography and digital imagery, and satellite data have been used to remotely detect brush and weeds on rangelands (Gausman *et al.*, 1977b; Richardson *et al.*, 1981; Carneggie *et al.*, 1983; Strong *et al.*, 1985; Everitt *et al.*, 1994; Lass *et al.*, 1996; Lass and Callihan, 1997; Everitt *et al.*, 2001a).

Over the past decade remote sensing, geographic information system (GIS), and Global Positioning System (GPS) technologies have been integrated for detecting and mapping the distribution of noxious rangeland plants (Dewey *et al.*, 1991; Anderson *et al.*, 1996; Everitt *et al.*, 1996; Everitt *et al.*, 2001a). Remote observations in georeferenced formats help to assess the extent of infestations, track changes, develop management strategies, and evaluate control measures on noxious plant populations.

Airborne Methods for Noxious Weed Detection

Scientists at the ARS Kika de la Garza Subtropical Agricultural Research Center (Weslaco, Texas) have conducted extensive research on using remote sensing technology for distinguishing noxious plant species on rangelands. Research has focused on describing the light reflectance characteristics of weed and brush species and utilizing remotely sensed imagery for their detection. Aerial photography has been the most used remote sensing technique for detecting plant species. Aerial photographs provide the finest spatial resolution and capture the spatial and textural essence of the scene with greater fidelity than any other procedure (Tueller, 1989).

Initial research at Weslaco on the utilization of remote sensing technology for detecting noxious plants was conducted by Gausman *et al.* (1977b). They described the light reflectance of silverleaf sunflower [*Helianthus argophyllus* Torr. & A. Gray] and demonstrated that aerial color-infrared (CIR) (0.50- to 0.90-μm) photography could be used to distinguish this annual weed on south Texas rangelands. The ability to remotely distinguish silverleaf sunflower was attributed to its white pubescent foliage that gave it higher visible (0.45- to 0.75-μm) reflectance than did other associated species.

The study on silverleaf sunflower stimulated further research using CIR aerial photography to detect false broomweed [*Xylothamia palmeri* (A. Gray) G. L. Nesom], broom snakeweed [*Gutierrezia sarothrae* (Pursh.) Britton & Rusby], and spiny aster [*Chloracantha spinosa* (Benth.) G. L. Nesom] (Everitt *et al.*, 1984; Everitt *et al.*, 1987; Anderson *et al.*, 1993). These three weedy sub-shrubs have erectophile (erect-leaf) canopy structures that produce various

dark brown to black image responses on CIR photographs that can be distinguished from the various shades of magenta, red, and light brown of other plant species (Plate 1). Figure 1 shows canopy reflectance data obtained for broom snakeweed and eight associated plant species and mixtures over the 0.45- to 0.90-μm spectral region. The visible (0.4- to 0.7-μm) reflectance of broom snakeweed was similar to that of several other associated species, but its near-infrared (NIR; 0.77- to 0.90-μm) reflectance was lower than that of the other species. The low NIR reflectance of broom snakeweed was due to it erectophile canopy structure (Everitt *et al.*, 1987).

One of the most important factors for distinguishing noxious species is obtaining the aerial photographs at the proper phenological stage, usual during flowering. Blackbrush [*Acacia rigidula* Benth.] and huisache [*Acacia farnesiana* (L.) Willd.] are two woody legumes that often create brush problems on Texas rangelands (Scifres, 1980). Both blackbrush and huisache flower concurrently in late February or March, producing a profusion of small cream to light yellow flowers and orange-yellow flowers, respectively, that encompass their entire canopies, giving each species a striking appearance. Aerial conventional color (0.40- to 0.70-μm) photography was used to distinguish blackbrush and huisache infestations. Plant canopy reflectance measurements on flowering blackbrush and huisache showed that they had higher visible reflectance than did other associated species (Everitt, 1985; Everitt and Villarreal, 1987). Conventional color photography has also been used successfully to distinguish common goldenweed [*Isocoma coronopifolia* (A. Gray) Greene] and Drummond goldenweed [*Isocoma drummondii* (T. & G.) Greene] during their flowering stages in the fall (Everitt *et al.*, 1992). These two weedy shrubs infest rangelands in southern Texas and northeast Mexico (Mayeux and Scifres, 1978; Mayeux and Scifres, 1981).

More recent research at Weslaco has shown that some noxious rangeland species can be remotely distinguished best in winter. Redberry juniper [*Juniperus pinchotii* Sudw.] is a troublesome evergreen shrub or small tree that invades rangelands in the southwestern United States. Everitt *et al.* (2001b) used CIR aerial photography for distinguishing redberry juniper infestations on the Texas Rolling Plains in winter due to its evergreen foliage. Other associated species that are confused with redberry juniper during the growing season are dormant in winter. Ground reflectance measurements supported these findings. Computer image analyses of a CIR photograph showed that redberry juniper infestations could be quantified, and an accuracy assessment of the classification had an overall accuracy of 89 percent.

In the past several years, videography has emerged as a remote sensing tool for natural resource assessment (Mausel, 1995; King, 1995). Videography has many attrib-

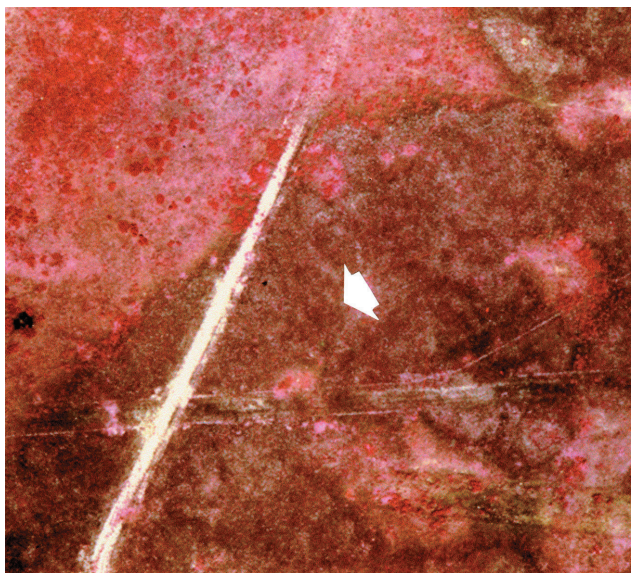

Plate 1. Color-infared photograph (original scale 1:10,000) of broom snakeweed near Tatum, New Mexico, in August 1984. The arrow points to the typical dark brown to black image of broom snakeweed.

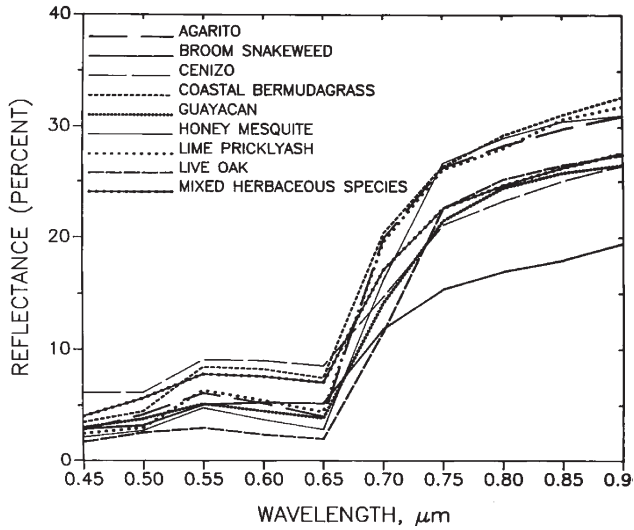

Figure 1. Field reflectance over the 0.45- to 0.90-μm waveband interval for broom snakeweed and eight other associated rangeland species or mixtures on south Texas rangelands in August 1984.

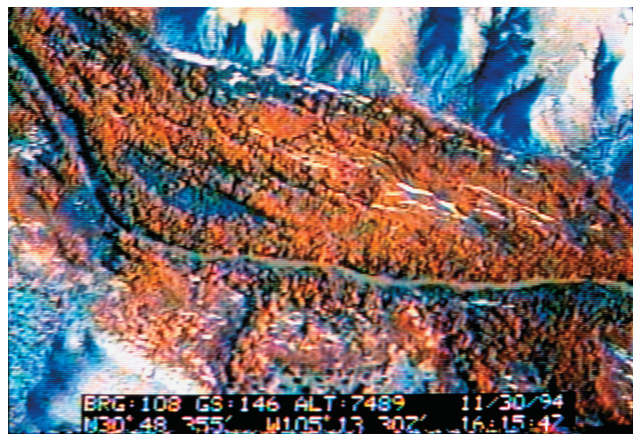

Plate 2. Conventional color video image of an infestation of saltcedar on the Rio Grande River near Candellaria, Texas. The image was obtained at an altitude above ground level of 1500 m in November 1994. Saltcedar has a conspicuous yellow-orange image tone. The GPS data appear at the bottom of the image.

utes that are attractive for remote sensing, including the timely availability of imagery, its electronic format that allows for the digital processing of the signal and its integration with GPS devices, and its low cost (Everitt *et al.*, 1995b). The main disadvantage of video is its low resolution relative to aerial photographs.

Researchers at Weslaco have focused on the integration of aerial video, GPS, and GIS technologies for detecting and mapping noxious rangeland plant species. Initial research in this area was on the woody legumes blackbrush and huisache (Everitt *et al.*, 1993b). Conventional color videography was used to detect blackbrush and huisache during their flowering stages in March. The GPS latitude-longitude data provided on the video imagery was integrated with GIS technology to georeference populations of blackbrush and huisache on a regional map of south Texas.

Airborne multispectral video, GPS, and GIS technologies have also been integrated to detect and map Big Bend locoweed [*Astragalus mollissimus* var. *earlei* (Greene x Rydb.) Tidestr.] populations on west Texas rangelands (Everitt *et al.*, 1994). Big Bend locoweed is a toxic, perennial weed that causes widespread poisoning of cattle, horses, and sheep (Sperry *et al.*, 1964; James *et al.*, 1980). This toxic weed could be easily detected on CIR and black-and-white NIR video imagery.

Weslaco scientists conducted a project using conventional color videography, GPS, and GIS technologies to detect and map saltcedar [*Tamarix chinensis* Lour.] infestations in the southwestern United States (Everitt *et al.*, 1996). Saltcedar, also known as Chinese tamarisk, is an invader of riparian areas in the southwestern United States and northern Mexico. Plate 2 shows a conventional color video image of a saltcedar infestation along the Rio Grande river in west Texas. The GPS data appear on the bottom of the image. Saltcedar has a conspicuous orange-brown image that is easily distinguished from other associated vegetation, soils, and water. The distinct signature of saltcedar was due to its foliage turning a yellow-orange to orange-brown color in late fall prior to leaf drop.

Figure 2 (upper right) shows a regional GIS map of extreme west Texas. The bold symbols along the left margin of the map represent GPS latitude-longitude coordinates obtained from video images of saltcedar populations along a portion of the Rio Grande. Areas with stars represent high populations of saltcedar, those with triangles have medium populations, and those represented by a plus sign have low populations. Population levels were assigned after a qualitative analysis of the video imagery of the area. Criteria for population levels were: greater than 50 percent cover, high; 25 to 50 percent cover, medium; and less than 25 percent cover, low. Each symbol represents a composite of two to three video scenes because of the small map scale. A detailed GIS map of an area with several high saltcedar populations is shown in the center left portion of Figure 2. The map in the lower left portion of Figure 2 provides more detail of roads and hydrography associated with the saltcedar populations.

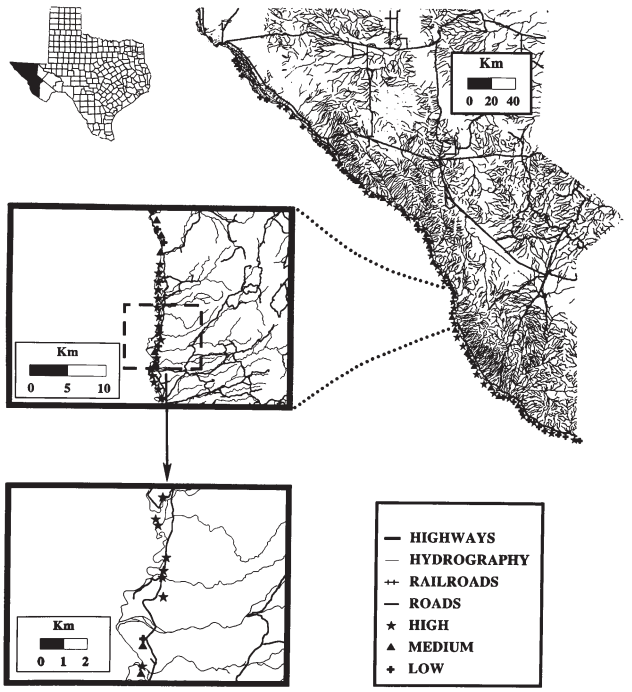

Figure 2. Regional GIS map (upper right) of extreme west Texas depicting GPS locations where saltcedar infestations occur along a portion of the Rio Grande River. The stars represent high populations of saltcedar, triangles are medium populations, and plus signs have low populations. Each symbol represents a composite of two to three video scenes because of the small detail of the map. A detailed map (left center) depicts an area with generally high populations of saltcedar. The lower left map shows even greater detail of the highly populated area.

Satellite Methods for Noxious Weed Detection

Although satellite imagery has been available for nearly 30 years, relatively few studies have reported its use for detecting noxious plants. The relatively coarse spatial resolution of satellite sensor data, as compared to aerial photography and videography, has limited its usefulness for this application. Nonetheless, satellite sensors have shown potential for detecting relatively large stands of weeds. Richardson *et al.* (1981), at ARS Weslaco, conducted a pilot study to assess Landsat multispectral scanner satellite data for detecting silverleaf sunflower infestations on Texas rangelands. They reported that this annual weed could be distinguished on CIR (bands 4, 3, and 2) Landsat imagery, which agreed with an earlier study using CIR film (Gausman *et al.*, 1977b). The geographic occurrence of silverleaf sunflower areas on a line-printer map generated from the Landsat image were in good agreement with their known aerial photographic locations.

Additional research at Weslaco in the 1990s showed the application of the French satellite SPOT (System Pour d'Observation de la Terre) for detecting noxious weeds. Anderson *et al.* (1993a) demonstrated that SPOT data could be used to detect major stands of false broomweed on south Texas rangelands. They also showed that infestations could be mapped, permitting acreage estimates of this weed over large areas. In another study, SPOT imagery was used to distinguish and quantify shin oak [*Quercus havardii* Rydb.] on northwest Texas rangelands (Everitt *et al.* 1993a). They also used low altitude videography to assist in interpreting the satellite data.

The Ecological Area-Wide Management (TEAM) of Leafy Spurge

In the 1990s, research began at the Northern Plains Agricultural Research Laboratory (Sidney, Montana) to evaluate the potential of using remote sensing technology for detecting leafy spurge [*Euphorbia esula* L.]. This research is part of the TEAM Leafy Spurge program, which is managed cooperatively with the USDA Animal and Plant Health Inspec-

tion Service (APHIS). Leafy spurge is an exotic weed that has created a severe range management problem in the Northern Great Plains of the United States and in the Prairie Provinces of Canada (Rees and Spencer, 1991). It infests approximately two million hectares of land in North America (Quimby and Wendel, 1997; Anderson *et al.*, 2003).

Initial research established that leafy spurge had higher visible reflectance than other associated species in early summer when it develops conspicuous yellow-green bracts. Leafy spurge could be remotely distinguished on both conventional color and CIR aerial photographs during this phenological stage (Everitt *et al.*, 1995a). Anderson *et al.* (1996) used high altitude conventional color aerial photography and GIS to map and quantify the extent of leafy spurge within the South Unit of Theodore Roosevelt National Park in southwestern North Dakota. The joint use of GIS and remote sensing provided previously unavailable information about the extent and spatial dynamics of leafy spurge within the park. More recently, Anderson *et al.* (1999) used aerial photography and GIS technologies to map and quantify the extent, distribution, and spatial-temporal dynamics of leafy spurge within a portion of the South Unit of Theodore Roosevelt National Park between 1993 and 1998. Anderson *et al.* (1999) found that leafy spurge had doubled in extent in five years, and the spatial distribution of the invasion over the landscape was highly predictable.

Because of the distinctive yellow-green bracts, current research from the Hydrology and Remote Sensing Laboratory (Beltsville, Maryland) on detection and mapping leafy spurge is focusing on the use of hyperspectral imagery (Figure 3). Parker Williams and Hunt (2002) showed that Airborne Visible Infrared Imaging Spectrometer (AVIRIS) data and new techniques for the analysis of hyperspectral data can be used to accurately map the amount of leafy spurge cover. These techniques, particularly mixture-tuned matched filtering, separate a single unique spectrum (called an endmember) from the background spectra based on signal processing technologies. One of the reasons for the excitement about using hyperspectral analysis is that small cover amounts (about 5 percent) can be detected even in community types such as woodlands, which is difficult because of the mixture of understory, shadows, and bright tree crowns (Parker Williams and Hunt, 2002). Additional work is being continued by TEAM Leafy Spurge at the Northern Plains Agricultural Research Laboratory with another hyperspectral sensor, the Compact Airborne Spectrographic Imager, CASI (Kokaly *et al.*, in press). Preliminary analyses of the data indicate that the use of hyperspectral imagery extends the period of time for detection of leafy spurge infestations beyond the two- to three-week window of maximum flowering required for detection by aerial photography.

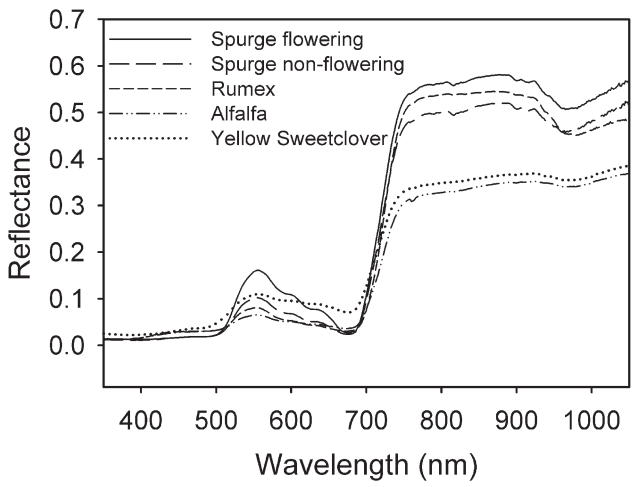

Figure 3. Spectral reflectance of various plants in northeastern Wyoming: Leafy spurge (*Euphorbia esula* L.) flowering and green non-flowering shoots, Curly dock (*Rumex crispus* L.), Yellow sweetclover (*Melilotus officinalis* Lam.) flowering shoots, and alfalfa (*Medicago sativa* L.) non-flowering shoots.

In conclusion, hyperspectral remote sensing is an extremely powerful method for detection of leafy spurge, but what about other invasive weeds? Ustin *et al.* (2002) show that hyperspectral remote sensing can pick up a spectrally unique iceplant (*Carpobrotus edulis*) as well as some other invasive weeds such as jubata grass (*Cordateria jubata*), fennel (*Foeniculum vulgare*), and giant reed (*Arundo donax*). The economic benefits from detection of invasive weeds is a compelling justification for an operational hyperspectral satellite.

Rangeland Productivity

Estimation of standing dry mass and yields was one of the earliest applications of satellite remote sensing for agricultural crops, and the developed techniques were applied early on to rangelands (Tucker *et al.*, 1975; Richardson *et al.*, 1983; Everitt *et al.*, 1986; Aase *et al.*, 1987; Anderson *et al.*, 1993b). At the time, field techniques for estimating productivity were based on measuring peak biomass, so estimation of productivity for rangelands was based on remote sensing peak biomass (Tucker *et al.*, 1983; Everitt *et al.*, 1989). Leaf area index (LAI) is related to mass of the foliage; the ratio between leaf area and leaf mass is the specific leaf area. Many studies examined the use of remote sensing for estimating LAI (Curran, 1983; Hatfield *et al.*, 1985; Price, 1993; Price and Bausch, 1995; Qi *et al.*, 2000c).

Some trends emerged, but also problems became apparent, which limits the usefulness of these approaches. One of the major limitations is that relationships between remotely sensed vegetation indices and either biomass and LAI are site specific, indicating that the soil background has strong effects on remotely sensed data (Ezra *et al.*, 1984; Huete *et al,* 1985; Huete, 1988; Price, 1993; Qi *et al.,* 1994; Price and Bausch, 1995). Multitemporal remote sensing (multiple acquisitions of the same target on different dates) is powerful because, in part, the soil background is constant. However, multitemporal data also allow more mechanistic models of plant production to be used.

Radiation Use Efficiency Models of Gross Primary Production

Radiation use efficiency is generally the amount of photosynthetic production per unit of radiation absorbed, with different operational definitions depending on specific situations and research objectives (Montieth, 1977; Kumar and Montieth, 1981; Sinclair and Horie, 1989; Sinclair and Muchow, 1999; Kiniry *et al.*, 1999). The efficiency of radiation use is defined as the mass of carbon uptake per absorbed photosynthetically active radiation (APAR; MJ^{-2} day^{-1}). Following Ruimy *et al.* (1995), gross primary production (GPP; g C m^{-2} $time^{-1}$) is summed over some time period from weekly to yearly: i.e.,

$$\text{GPP} = \varepsilon \sum \text{APAR} \qquad (1)$$

where ε is the efficiency of radiation use (g C MJ^{-1}). Often APAR is approximated by either intercepted photosynthetically active radiation (PAR) or intercepted solar radiation (Prince, 1991; Running and Hunt, 1993; Gower *et al.*, 1999).

Frequently, radiation use efficiency may be defined using the mass of dry matter rather than the mass of carbon, incorporating ash weight into the value of ε. Furthermore, radiation use efficiency is often determined using either net primary production (NPP) or above-ground net primary production (ANPP); thus, autotrophic respiration and carbon allocation are incorporated in the value of ε (Prince, 1991; Hunt and Running, 1992; Running and Hunt, 1993; Hunt, 1994; Ruimy *et al.*, 1994; Gower *et al.*, 1999; Goetz and Prince, 1999).

For ideal growth conditions, differences of ε will be related to the maximum photosynthetic rates of vegetation, which can be estimated from land-cover type. For actual growth conditions, ε will be reduced from the maximum because (1) stomatal closure caused by drought, high vapor pressure differences between leaf and air, night-time temperatures falling below freezing, and ozone pollution; and (2) stresses affecting photosynthetic rate. Furthermore, Ruimy *et al.* (1995) concluded that ε is reduced, usually by about 50 percent, from the photosynthetic capacity of the foliage being light saturated (*cf.* Goetz and Prince, 1999).

The direct physical quantity estimated from the normalized difference vegetation index (NDVI) is the fraction of absorbed to incident photosynthetically active radiation (f_{APAR}, dimensionless). The NDVI is defined as

$$\text{NDVI} = (\text{NIR} - \text{Red})/(\text{NIR} + \text{Red}) \quad (2)$$

where NIR is the spectral radiance from a near-infrared band and Red is the spectral radiance from a red band. Originally, NDVI was developed to enhance the signal from vegetation and to reduce the effects of atmospheric transmittance, topography, and solar elevation and azimuth (Rouse *et al.*, 1974). Subsequently, Asrar *et al.* (1984), Hatfield *et al.* (1984), and others showed that NDVI was approximately equal to f_{APAR}, so APAR is estimated by the product of NDVI and daily incident PAR. Corrections are made to more accurately estimate f_{APAR} from NDVI (Goward and Huemmrich, 1992; Myneni and Williams, 1994).

Advanced Very High Resolution Radiometer (AVHRR) NDVI are most often used because these data are collected daily and composited over a short period, weekly or biweekly, to generate a mostly cloud-free image, so the change in f_{APAR} over a season may be determined. AVHRR NDVI shows the spatial distribution of vegetation response to changes in precipitation over large areas (Millington *et al.*, 1994; Liu and Kogan, 1996; Yang *et al.*, 1998). With the launches of the National Aeronautics and Space Administration's (NASA) Terra satellite in December 1999 and Aqua satellite in May 2002, the Moderate-Resolution Imaging Spectroradiometer (MODIS) is now providing improved estimates of f_{APAR} (Reeves *et al.*, 2001). More importantly, AVHRR data have been archived for a long period by the United States Geological Survey EROS Data Center (Sioux Falls, South Dakota), so the effects of the large year-to-year variability of rainfall can be averaged.

Scientists with the Hydrology and Remote Sensing Laboratory (Beltsville, Maryland) have shown that AVHRR NDVI data are useful for policy and economic analyses, because large areas are covered with large 1-km^2 pixels. On the other hand, these data are at too coarse a scale for stocking individual grazing allotments. Scientists with the Southwest Watershed Research Center (Tucson, Arizona) are applying radiation use efficiency models with Landsat Thematic Mapper data (30-m by 30-m pixels) for site-specific or precision ranching.

Estimation of Stocking Rate from High-Temporal-Resolution Satellites

One of the most important decisions of rangeland managers is setting the stocking rate for various kinds of livestock (cattle, sheep, goats, horses, etc.) with consideration for the requirements of coexisting wildlife (Holecheck, 1988; Briske and Heitschmidt, 1991). Holecheck (1988) set out an algorithm that can be used to determine the stocking rate based on ANPP. Remotely sensed GPP, determined from radiation use efficiency models, serves as the starting point for spatially distributed estimates of ANPP (Figure 4).

AVHRR data for the state of Wyoming were acquired from the EROS Data Center for 1990 through 1999. These data are similar to the Conterminous U.S. AVHRR Data Sets (Eidenshink, 1992), with the exception that the composites for 1998 and 1999 were done weekly instead of biweekly. Daily solar irradiances (MJ^{-2} day^{-1}) were calculated from National Weather Service meteorological data using a model by Winslow *et al.* (2001). Incident PAR were calculated from the weekly-average of solar irradiance multiplied by the fraction of PAR to solar radiation (measured to be 0.44 $\pm$ 0.04). Incident PAR was multiplied by f_{APAR} calculated from the NDVI data to calculate APAR; when NDVI data were not available, GPP was assumed to be zero.

Other data are needed as well, which are incorporated into a GIS: land-cover type, digital elevation data, climate data (incident PAR, temperature, and precipitation), and distance to water (Figure 4). Land cover was from the U.S. Geological Survey (USGS) EROS Data Center's Seasonal Landcover dataset (Eidenshink and Fuandeen, 1994). Autotrophic respiration was assumed to be 50 percent of GPP (Landsberg and Waring, 1997); allocation above ground was 50 percent for agriculture, shrubs, and forests and 20 percent for grasslands. The ANPP estimates by the method are shown in Plate 3.

Digital elevation model (30-m by 30-m) data were used to calculate slope for each pixel. The median value calculated for each 1-km^2 was determined and used to define the slope class. Slope class reductions are none for median slopes $\leq$10 percent, 30 percent for slopes from 11 to 30 percent, 60 percent for slopes from 31 to 60 percent, and 100 percent for slopes $\geq$61 percent. Utilization of ANPP was set at 5 percent for forests, 25 percent for shrubs, and 40 percent for grasslands and agriculture. After the reductions for slope and utilization, ANPP is converted to stock-

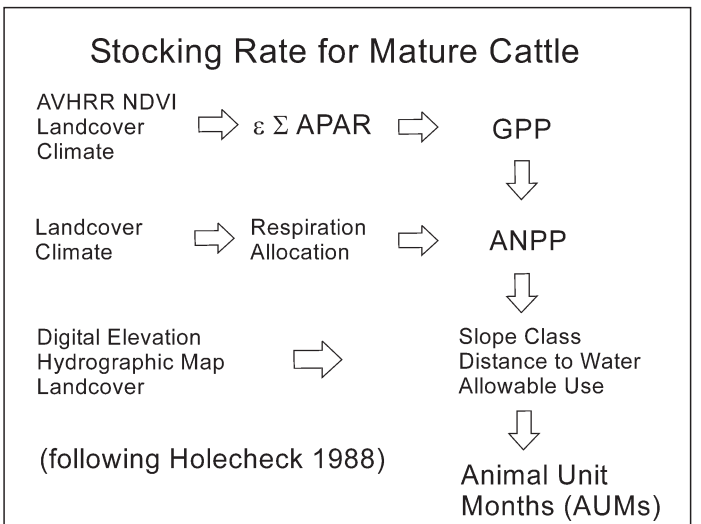

Figure 4. Flow diagram using Advanced Very High Resolution Radiometer (AVHRR) Normalized Difference Vegetation Index (NDVI), simple ecosystem models, and geographic theme data to calculate stocking rates based on algorithm of Holecheck (1988).

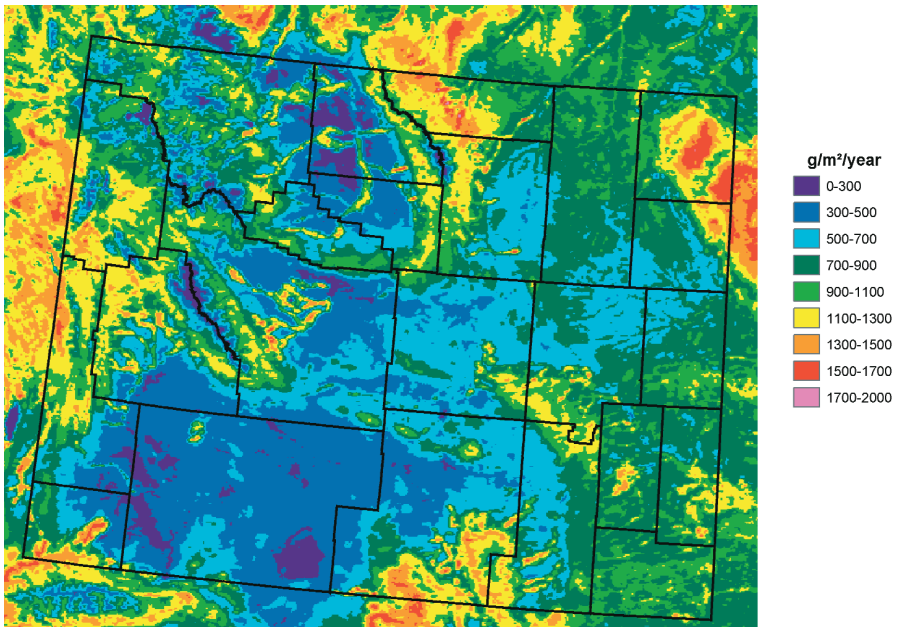

Plate 3. Above-ground net primary production (ANPP) for the state of Wyoming. AVHRR NDVI data from 1990 to 1999 were used to calculate the mean gross primary production (GPP), based on land-cover type and climate. Autotrophic respiration and allocation above ground were estimated as fractions of GPP determined from land-cover type. Dry matter is about 45 percent carbon.

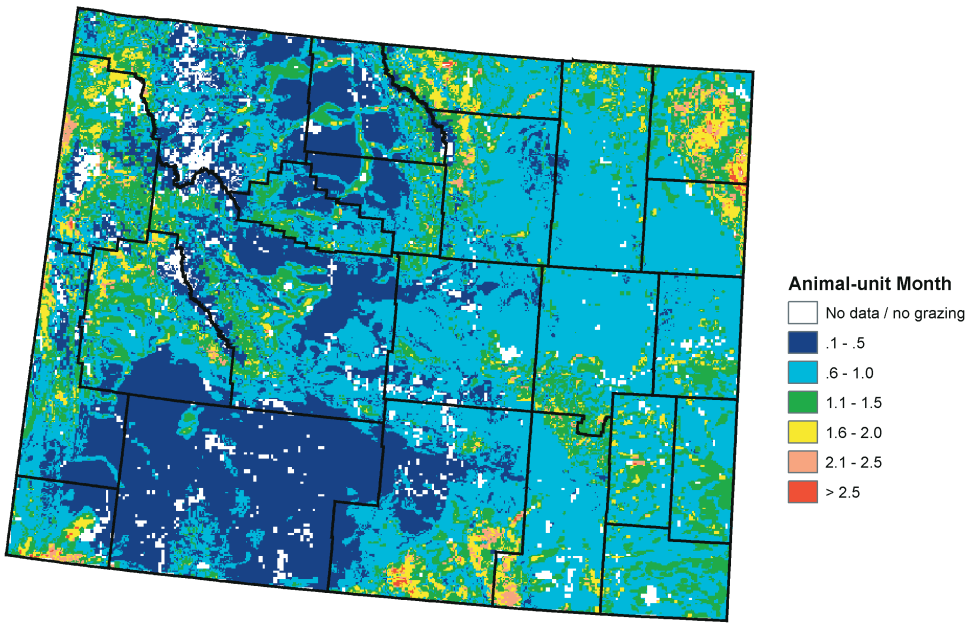

Plate 4. Stocking rates in Animal Unit Months (AUM) for the state of Wyoming. The AUM is based on a dry matter intake of 20 lbs (9.1 kg) per day for one mature cow (Holecheck, 1988). ANPP was reduced according to slope class and the utilization was set by land-cover type.

ing rates in Animal Unit Months or AUMs (Plate 4) based on the conversion in Holecheck (1988).

The problem of using such large pixels, such as with AVHRR or MODIS, is that each pixel is a mixture of sites with good forage and sites with little or no forage. It will be extremely difficult to test calculations of stocking rate based on such large pixels. If the relationship between NDVI and f_{APAR} is approximately linear (Goward and Huemmrich,

1992; Myneni and Williams, 1994), and ε is determined primarily by climate, then pixel GPP and ANPP are spatial averages of the GPP and ANPP on the ground. If a pixel shows that the number of AUMs is 1.0, but the rancher or range conservationist know that the sustainable AUMs for a specific allotment in that pixel is say 3.0, then the other allotments in that pixel must have a much lower number of AUMs to obtain the pixel average.

Rangeland Productivity from Landsat Data

Radiation use efficiency models are essentially scale independent; the spatial scale of the output is dependent on the spatial scale of the inputs. Scientists at the Southwest Watershed Research Center (Tucson, Arizona) have developed radiation use efficiency models for use with Landsat data (Nouvellon *et al.*, 2000; Nouvellon *et al.*, 2001). The pixel size is 30 meters, or 900 m^2, about 0.1 percent of an AVHRR pixel. Data from the Thematic Mapper (TM; Landsats 4 and 5) and the Enhanced Thematic Mapper Plus (ETM+; Landsat 7) are suitable for rangeland management because the 20-year time series of these data can be averaged to overcome the high year-to-year variation from rainfall. With Landsat Multispectral Scanner (MSS; Landsats 1 through 5) data, the time series of data extends to 30 years. Washington-Allen *et al.* (1999) is using the long time series to examine plant community changes in relation to climatic variability.

At the ARS Walnut Gulch Experimental Watershed in southeastern Arizona, high-spatial, low-temporal scale, visible remote sensing data were used to calibrate an ecosystem model for semi-arid perennial grasslands (Nouvellon *et al.*, 2000; Nouvellon *et al.*, 2001). The model was driven by daily meteorological data and simulated plant growth and water budget on the same time step. The model was coupled with a canopy reflectance model to yield the time course of shortwave radiometric profiles. Landsat TM and ETM+ images from ten consecutive years were used to refine the model on a spatially distributed basis over a semiarid grassland watershed (Plate 5). The lower elevations of the watershed (western side) are desert shrubs and were excluded from the analyses. The higher elevations of the watershed (eastern side) are comprised of C_4 warm-season grasses: black grama [*Bouteloua eriopoda* (Torr.) Torr.], curly mesquite [*Hilaria belangeri* (Steud.) Nash], hairy grama [*Bouteloua hirsuta* Lag.], blue grama [*Bouteloua gracilis* (Kunth) Lag. ex Griffiths], and sideoats grama [*Bouteloua curtipendula* (Michx.) Torr.] (Weltz *et al.*, 1994). The predicted aboveground biomass (Plate 5) was compared to the measured biomass; generally, the model predicted within a root-mean-square error of 12.2 g dwt m^{-2} (Nouvellon *et al.*, 2001). Results showed that this approach could provide spatially distributed information about both vegetation and soil conditions for day-to-day grassland management. Furthermore, only one or two images per year were required to calibrate the model, thus overcoming the common limitation of infrequent and/or cloudy image acquisitions.

The Rangeland Analysis utilizing Geospatial information Science (RANGES) project is another effort to estimate productivity on grasslands using Landsat data, centered at the Southwest Watershed Research Center. Collaborators are the ARS Great Plains Systems Research Unit (Fort Collins, Colorado), Michigan State University (East Lansing, Michigan), and Veridian (Ann Arbor, Michigan). NASA's Commercialization Remote Sensing Program funds the project, with the objective of prototyping and commercializing operational tools from remote sensing for rangeland management. After the summer rainy season, rangeland managers are provided with layers of data showing mesquite and evergreen canopy cover, herbaceous cover, height, and biomass. Software provided with the data can calculate available forage within pasture boundaries or polygons of interest to plan the intensity and timing of grazing. If there is sufficient interest, a second layer of data could be provided just before the next summer rainy season to estimate utilization.

The primary technical problem RANGES faced was the difficulty of estimating the biomass of senescent grass. Images collected during the summer rainy season are often obscured by clouds, and the grasses senesce soon after the rains stop. A normalized difference senescent vegetation index, or NDSVI, was developed that used a shortwave-infrared band rather than NIR as in the NDVI (Qi *et al.*, 2000a). Canopy cover is calculated from NDVI (Qi *et al.*, 2000b). Empirical relationships based on field data are used to estimate height and to adjust biomass estimates made by multiplying the cover and the height. To date, the focus of the project has been on grasslands, but methods of estimating forage in areas with significant shrub or tree canopies are also needed. Commercialization of the RANGES products will depend on demand; the cost of the products would vary on the order of 5 to 10 cents per hectare in 2002.

Airborne Lidar Technology for Measuring Rangeland Properties

Land surface features (i.e., vegetation, topography, surface roughness) influence the functions of rangeland landscapes. Measuring these features and their spatial distribution using conventional ground-based technologies provides limited temporal and spatial data. Lidar technology from airborne platforms provides rapid and accurate data of land surface topography, roughness, vegetation features, and patterns. Airborne lidar has been used to measure vegetation properties (Ritchie *et al.*, 1992; Ritchie *et al.*, 1993a), erosion features (Ritchie *et al.*, 1993b), topography (Krabill *et al.*, 1984), and aerodynamic roughness (Menenti and Ritchie, 1994).

Airborne lidar data have been collected over rangelands in the western United States by the Hydrology and Remote Sensing Laboratory (Beltsville, Maryland), in cooperation with ARS rangeland research locations and various Long-Term Ecological Research (LTER) research sites (Ritchie *et al.*, 2001). Examples are given of applications of airborne lidar data for measuring rangeland properties.

Landscape and vegetation patterns associated with a 100-m lidar profile from the ARS Reynolds Creek Watershed (Boise, Idaho) are shown in Figure 5. Topography, roughness, and gaps between the vegetation elements are shown in Figure 5a. The elevation of the ground surface under the vegetation is estimated by assuming that minimum elevation measurements along the profile represent lidar measurements that reached the ground surface. If the topography (oriented roughness) is removed by calculating the difference between the estimated ground surface and the actual lidar measurements, vegetation heights and distribution and surface roughness can be calculated (Figure 5b). These measurements are used for estimates of vegetation canopy height. This height data can be used to calculate canopy cover. Using all data, the average vegetation height for this 100-m segment is 0.47 ± 0.73 m. Using measurements greater than 0.5 m, the average vegetation height is 1.77 ± 0.99 m.

Lidar profiles and ground data were collected from five different vegetation types in the ARS Reynolds Creek Watershed (Clark *et al.*, 2001): mountain big sagebrush [*Artemisia tridentata* Nutt. subsp. *vaseyana* (Rydb.) Beetle], low sagebrush [*Artemisia arbuscula* Nutt.], Wyoming big sagebrush [*Artemisia tridentata* Nutt. subsp. *wyomingensis* Beetle & A. L. Young], bitterbush [*Purshia tridentata* (Pursh) DC.], and greasewood [*Sarcobatus vermiculatus* (Hook.) Torr.] (Table 1). The ground data are an average of six 30-m transects along an approximate 1-km line using the line inter-

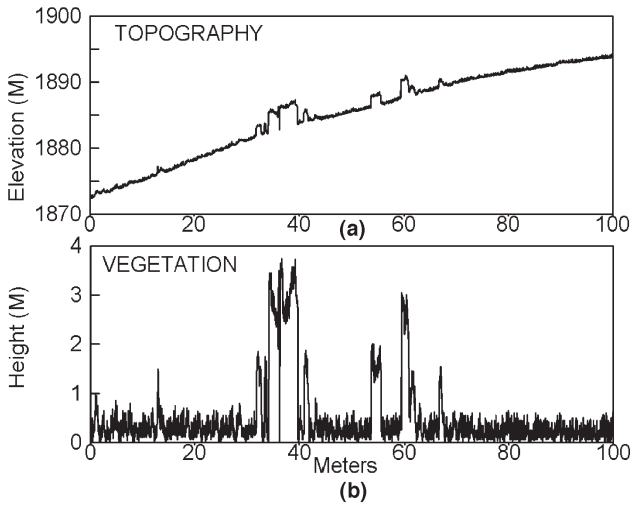

Figure 5. Airborne laser measurements of (a) landscape features and (b) vegetation heights for a 100-meter section of Reynolds Creek Watershed, near Boise, Idaho.

cept method. The lidar data are an average of three 1-km transects over the same area. The difference in the average heights between the ground and lidar measurements of the transects ranged from 2.0 to 8.7 cm with the lidar measured heights always being lower. There was no statistical difference between the ground and lidar height measurements at the 5 percent level of probability.

Studies in a south Texas mesquite [*Prosopis glandulosa* Torr.] stand at the ARS Kika de la Garza Subtropical Agricultural Research Center (Ritchie *et al.*, 1992) and a desert rangeland in the ARS Walnut Gulch Experimental Watershed (Weltz *et al.*, 1994) have shown that the lidar measurements of vegetation heights and cover were highly correlated with ground measurements made with standard line intercept techniques.

Large landscape features can also be quantified to estimate their effects on water flow and quality across the landscape. The valley and channel associated with Reynolds Creek near the outlet of the ARS Reynolds Creek Experimental Watershed (Figure 6) were measured using two seconds of airborne lidar data. The profile shows a 140-m cross section of the valley with the channel. The channel cross section under the lower dashed line was calculated to be 48.9 m^2. Other stages for water flow could be assumed

TABLE 1. COMPARISON OF GROUND AND LASER PROFILER MEASUREMENTS OF COVER AND HEIGHT FOR FIVE PLANT COMMUNITIES IN THE ARS REYNOLDS CREEK WATERSHED.

Site	Plant Name[1]	Plant Cover[2] Ground (%)	Plant Cover[3] Laser (%)	Plant Height[2] Ground (cm)	Plant Height[3] Laser (cm)
Mountain Big Sagebrush	Total Vegetation	86.3	76.0[4]	37.5 ± 17.8	34.2 ± 18.4
	ARTRV	56.0	69.7[5]		
	SYOR	4.0			
	Forbs	20.3			
	Grass	6.0			
	Ground	13.7			
Low Sagebrush	Total Vegetation	54.3	60.4	19.7 ± 13.2	17.7 ± 15.2
	ARAR	38.0	49.7		
	Forbs-Other	4.3			
	Grass	12.0			
	Ground	45.7			
Wyoming Big Sagebrush	Total Vegetation	32.3	79.5	38.1 ± 21.1	32.1 ± 13.9
	ATTRW	23.5	74.0		
	SAVE	2.2			
	Forbs-other	3.9			
	Grass	2.7			
	Ground	67.7			
Bitterbrush	Total Vegetation	75.9	79.8	45.5 ± 30.1	36.8 ± 18.3
	ARTTW	25.0	74.4		
	PUTR	15.5			
	Forbs-other	14.2			
	Grass	21.2			
	Ground	24.1			
Greasewood	Total Vegetation	51.5	69.1	40.5 ± 22.3	32.35 ± 11.9
	SAVE	16.8	61.8		
	ARTRW	12.8			
	Forbs-other	14.4			
	Grass	7.5			
	Ground	48.5			

[1] Vegetation
ARTRV-Mountain Big Sagebrush-[Artemisia tridentata subsp. vaseyana (Rydb.) Beetle]
SYOR-Snow Berry-[Symphoricarpos oreophilus A. Gray]
ARAR-Low Sagebrush-[Artemisia arbuscula Nutt.]
ATTRW-Wyoming Big Sagebrush-[Artemisia tridentata subsp. wyomingensis Beetle & A. L. Young]
SAVE-Greasewood-[Sarcobatus vermiculatus (Hook.) Torr.]
PUTR-Bitterbrush-[Purshia tridentata (Pursh) DC.]
[2] Average of six 30-m ground transects along an approximate 1-km line
[3] Average of three 1-km laser transects over approximately the same line as the ground transects
[4] Percent cover for all laser measurements
[5] Percent cover for laser measurements greater than 15 cm above the ground surface

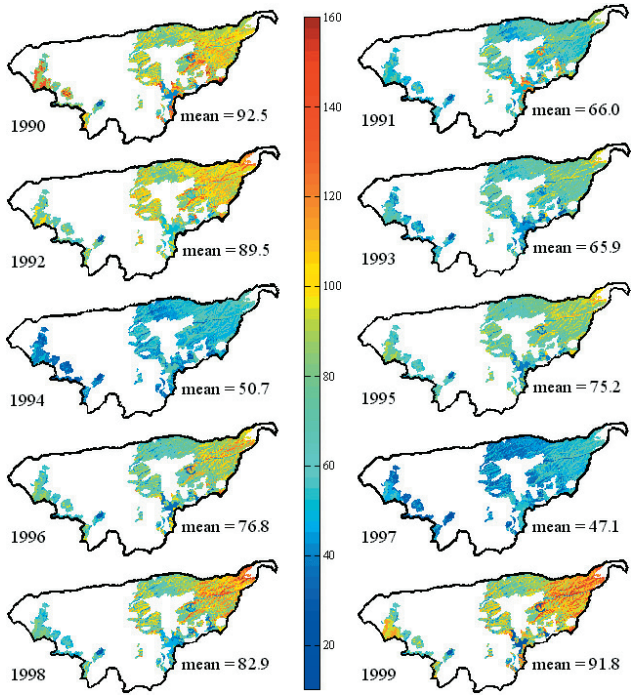

Plate 5. Annual net primary production (g dwt m^{-2} $year^{-1}$) of grasslands at the ARS Walnut Gulch Experimental Watershed. Remote sensing inputs from the Landsat (4 and 5) Thematic Mapper and Landsat 7 Enhanced Thematic Mapper Plus are coupled with climate and other data in an ecosystem model based on radiation use efficiency.

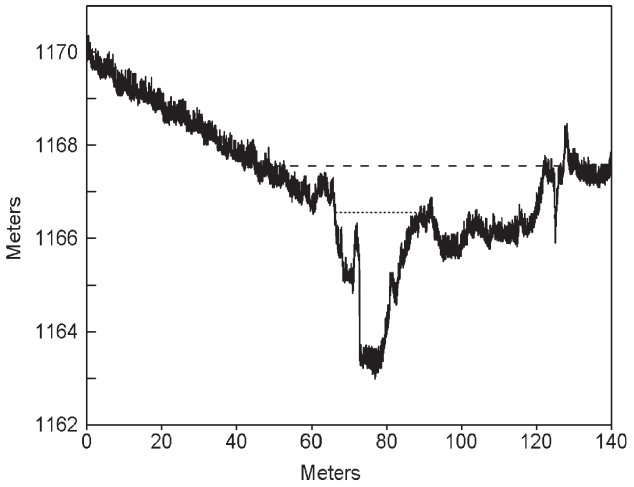

Figure 6. Cross section measured by a laser altimeter of Reynolds Creek. The dotted line represents the top of the channel and the dashed line represents the flood plain. Area of the channel under the lower dotted line is 48.94 m^2.

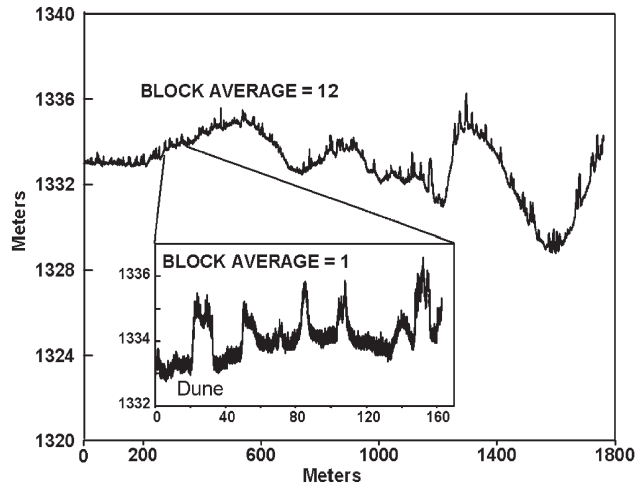

Figure 7. Topographic profile measured using an airborne laser altimeter of dunes at the Jornada Experimental Range near Las Cruces, New Mexico. The long profile was made by block averaging 12 laser measurements; the short profile is not averaged.

(Figure 6, upper dashed line) and their cross sections measured to estimate channel/flood plain capacity. Channel/flood plain roughness can be measured to help calculate resistance to flow and potential flood area at different stages. Cross sections of channels and gullies have been measured at rangeland sites in Arizona and Oklahoma (Ritchie *et al.*, 1993b; Ritchie *et al.*, 1995) to quantify gully, channel, and flood plain roughness, and cross sections. Data on gully, channel, and flood plain cross sections, roughness, and degradation provide valuable data for the design and development of physical structures to control flow, reduce bank erosion, and to calculate flows and areal extent of floods.

Airborne lidar altimeters can be used to measure longer topographic profiles quickly and efficiently. At an airplane ground speed of 75 m per second, 4.5-km profiles are measured each minute (240,000 lidar measurements) with the same detail as shown for short profiles. An example of a topographic profile of a mesquite coppice dune area at the ARS Jornada Experimental Range (Las Cruces, New Mexico) is shown in Figure 7 using approximately 25 seconds of the lidar altimeter data. The profile is from an area with mesquite shrubs on top of the dunes and almost no vegetation between the dunes (Ritchie *et al.*, 1998). The insert in Figure 7 is the full resolution lidar data (no averaging) showing 1- to 3-m tall dunes with vegetation on them.

The profile shown in Figure 7 illustrates the topographic data that can be collected with the lidar. While the length of the profile shown is 1.8 km, profiles can be measured and analyzed for any length. Greater spatial and vertical detail on such profiles can be measured by using smaller block averages or all data points (Figure 7, insert). Ease and speed of data collection allow measurement of several profiles over the same area with a minimum of extra survey cost. Such measurements of topography provide data for estimating aerodynamic roughness for understanding water and wind flow across the landscape (Menenti and Ritchie, 1994).

While profiling lidars provide two-dimensional cross sections of topographic and vegetation features which allow quantification of the landscape morphology, scanning lidars can provide measurements of three-dimensional shapes and areal distributions of landscape features. Scanning lidar data of a shrub-coppice dune area in the desert grasslands of the ARS Jornada Experimental

Range was used to measure the morphological characteristics (height, perimeter, distribution) of coppice dunes with acceptable accuracy and precision for a range of uses. Comparable ground-based measurements would be time-consuming if not impossible to collect. Scanning lidar data used in conjunction with land-cover classification from multispectral aerial videography or spectral scanners provide improved information on both the areal and the vertical variability of these dunes. The use of such systems together is highly synergistic (Rango *et al.*, 2000), and provides data on the spatial distribution of the dunes that is necessary for understanding the patterns of dune development and movement.

Fractal analysis of 100,000 lidar measurements (~2 km in distance) for 15 lidar transects at the ARS Reynolds Creek Experimental Watershed (three transects for each of the five vegetation types in Table 1) were used to calculate the root-mean-square (RMS) roughness known to display fractal scaling along the cross sections of self-affine surfaces (Pachepsky *et al.*, 1997; Pachepsky and Ritchie, 1998). Root-mean-square roughness is the RMS value of residuals of a linear trend fitted to the sampled points in an interval. The interval is called a "window." Construction of the fractal models for a line includes (1) the selection of a property to be calculated on different scales, (2) the selection of a procedure to define ranges of scales within which the self-affinity exists, and (3) the selection of a method to calculate fractal dimensions for each range of the self-affinity. To define ranges of scales over which self-affinity exists, the linearity measure introduced in fractal modeling by Yokoya *et al.* (1989) was calculated.

Results of applying the linearity measure to separate different ranges of fractal scaling on roughness plots are shown in Figure 8. Each vegetation type (Table 1) had a unique fractal pattern. Fractal dimensions between 0.80 and 1.30 correspond to low irregularity. The low sagebrush, the shortest community, had the lowest fractal dimension, indicating a relatively uniform ground pattern. The greasewood and Wyoming big sagebrush had the higher fractal dimensions, indicating more irregularity and clumped patterns. These analyses indicate that separation of different vegetation types may be possible using fractal analysis of lidar data.

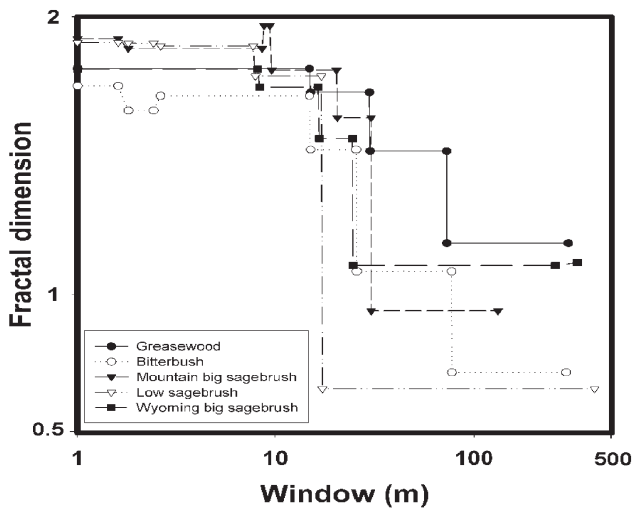

Figure 8. Intervals of linearity and fractal dimensions estimated by applying the linearity measure of Yokoya *et al.* (1989) to the dependencies of root-mean-square roughness on the window size for the airborne laser profiler data collected over the five different vegetation communities at the Reynolds Creek Watershed.

Airborne lidar altimetry can provide rapid quantification of landscape topography, gully and stream cross sections, and roughness and vegetation canopy properties of rangelands. Land surface roughness due to the physical and biological properties and features can be separated and quantified. These properties and features are integral parts of the landscape and have to be evaluated at large scales to understand the hydrology of rangeland systems. Measurements of these micro and macro surface features contribute to quantification of water retention, infiltration, evaporation, and movement from landscape surfaces and in channels and across flood plains. Channel and gully development, degradation, and roughness can be measured and used to estimate soil loss and explain water quality and flow patterns. Measurements of canopy properties and distribution across the landscape and their effect on water movement and aerodynamic roughness allow better understanding of evaporative loss, infiltration, and surface water movement. Scaling properties of lidar data provide compact indexes to compare and discriminate landscapes, as well as to summarize roughness properties for further applications. Airborne lidar altimeters offer the potential to measure rangeland properties over large areas quickly and easily. Such measurements will improve our understanding of the effects of these factors on hydrological systems of rangelands so that improved management practices and structures can be developed to manage our natural resources better.

Soil, Residue, and Plant Cover

One of the most important factors affecting soil erosion is the amount of exposed bare soil, which is negatively related to the cover of vegetation and residue. Vegetation indices, such as NDVI (Equation 2), not only are correlated with LAI, biomass, and f_{APAR}, but are also highly correlated to plant cover. However, differences in soil background can cause a large variation in vegetation indices for the same amount of cover or biomass, necessitating corrections in vegetation indices (Huete *et al.*, 1985; Huete, 1988; Qi *et al.*, 1994; Qi *et al.*, 2000c). Because cover and productivity are different and separate indicators of rangeland health, one vegetation index is insufficient. ARS scientists are examining sensors with better spatial and spectral detail, so that remote sensing can provide the necessary data for rangeland assessment and monitoring.

Hyperspectral Image Analysis

Hyperspectral data refers to imagery with a large number of contiguous, narrow wavebands so that each pixel of an image has its own reflectance spectrum; the premiere hyperspectral sensor is the Airborne Visible Infrared Imaging Spectrometer (AVIRIS) (Green *et al.*, 1998). The advantage of these data are that the cover of plants, litter, and soils can be separated with a technique of spectral endmember unmixing (Roberts *et al.*, 1998; McGwire *et al.*, 2000).

At the ARS Central Plains Experimental Range, operated by the ARS Rangeland Resources Research Unit (Fort Collins, Colorado and Cheyenne, Wyoming), AVIRIS imagery was acquired over a long-term grazing study (Hunt, 2003). Plant cover, primarily blue grama grass [*Bouteloua gracilis* (Kunth) Lag. ex Griffiths], estimated by spectral endmember unmixing was equal among treatments (Figure 9) and equal to measured plant cover on the ground for light, medium, and heavy grazed half-section pastures. Furthermore, the cover of shadow was proportional to the cover of shrubs.

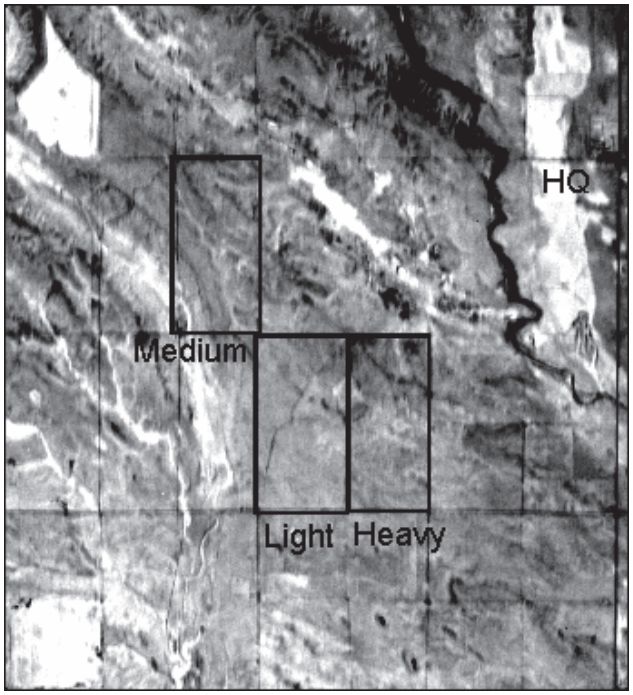

Figure 9. Fraction of the vegetation endmember from Airborne Visible Infrared Imaging Spectrometer (AVIRIS) acquired at the ARS Central Plains Experimental Range (CPER), near Nunn, Colorado. There are three long-term, continuous grazing treatments covering 0.5 square-mile half sections: heavy, medium, and light. Furthermore, there are large 50-m by 50-m exclosures to prevent grazing by large herbivores and livestock. There are no differences in mean plant cover among the treatments, and no difference in mean fraction of the vegetation endmember.

At red and near-infrared wavelengths, plant residue or litter is hard to separate from soil and does not interfere with vegetation indices for living plant biomass (Frank and Aase, 1994). During senescence, foliage loses water, exposing the chemical absorption features of leaf chemical constituents, which are detectable in the shortwave infrared region. The cellulose absorption index was developed to estimate residue cover using hyperspectral remote sensing (Daughtry, 2001; Daughtry *et al.*, 2002). Thus, full spectral unmixing is not necessary if additional wavebands are added to multispectral sensors, in order to create new indices which separate bare soil from residue.

Very Large Scale Aerial Imagery

Scientists at the High Plains Grassland Laboratory (Cheyenne, Wyoming), are measuring the amount of bare ground as a potential key attribute of rangeland health. Very large scale aerial (VLSA) imagery is being investigated as a means for inexpensive acquisition of statistically adequate, unbiased, high spatial resolution imagery from which to make accurate ground-cover measurements. The goal is the capture and interpretation of 1:50- to 1:200-scale imagery. The remote-sensing platform is an ultralight, three-axis airplane (Figure 10) with a laser altimeter for precise, instantaneous measurements of altitude. The sensors are high-shutter-speed film and digital cameras, which are automatically triggered by a computer using preprogramed coordinates with an interfaced GPS receiver.

Figure 10. Ultralight airplane used for very-large-scale aerial photography. The sensors are high-shutter-speed film and digital cameras, which are automatically triggered by a computer with an interfaced GPS receiver.

The system also provides the pilot with navigational information including ground speed, a critical parameter for close-to-the-earth photography.

Methods for making bare-ground measurements include manual photogrammetry and digital image processing (color density slicing image analysis). The latter effort is cooperative with the ARS Kika de la Garza Subtropical Agricultural Research Center (Weslaco, Texas). Ground data collected for comparison with aerial images includes cover data collected using laser-bar point frames (paper in preparation) and overhead, stereo, photography from 2 m above ground level. This ground photography is being analyzed using the same methods as for aerial imagery with the addition that stereo viewing is being tested for incorporation into supervised classification procedures for image analysis.

Algorithm Development

Research into remote sensing provides the knowledge base for future applications. However, research in remote sensing often requires extensive ground validation data ("ground truth"), which are expensive to obtain over large areas. Field experiments are generally conducted with multiple objectives so that synergistic interactions among different remotely sensed datasets may be studied. ARS scientists have been involved in initiating, planning, and conducting field experiments, usually with extensive collaboration among universities and other federal agencies (i.e., NRCS, NASA, USGS, the National Oceanographic and Atmospheric Administration, and the Department of Energy).

Many of these field experiments have been conducted in rangelands, and may point out future methods for rangeland monitoring, even though the development of practical remote sensing applications was not an experimental objective. The ARS Walnut Gulch Experimental Watershed, operated by the Southwest Watershed Research Center (Tucson, Arizona), was the site of the Monsoon '90 (Schmugge *et al.*, 1993; Kustas and Goodrich, 1994; Moran *et al.*, 1994), Walnut Gulch '92 (Moran *et al.*, 1996), and SALSA experiments (Goodrich *et al.*, 2000). The ARS Jornada Experimental Range (Las Cruces, New Mexico) hosted the Jornada Experiment, JORNEX (Rango *et al.*, 1998; Havstad *et al.*, 2000). Finally, the ARS Grazing Land Research Laboratory (El Reno, Oklahoma), which operates the Little Washita River Watershed, was the host for Washita '92 (Jackson *et al.*, 1995), Washita '94, Southern Great Plains Experiment '97 (Jackson *et al.*, 1999), and the Southern Great Plains Experiment '99. Other ARS experimental watersheds and rangeland experimental sites have also been used for remote sensing research, but not for such extensive multidisciplinary experiments.

Most of the research previously conducted for remote sensing applications is based on reflected solar radiation, with bands in the visible, near-infrared, and shortwave infrared wavelength regions. Two other wavelength regions are used in remote sensing, thermal infrared and microwave. Thermal infrared is used to determine land surface temperature, which is affected by the loss of latent heat by transpiration and evaporation. Microwave wavelengths can be remotely sensed by either passive or active sensors; water has a very strong dielectric constant, and therefore affects strongly the emission or backscatter, respectively, of microwaves.

Microwave Imagery for Soil Moisture Content

Microwave remote sensing provides information on water content of the target. By selecting the wavelength, it is possible to define the moisture condition of the atmosphere (short wavelengths), vegetation (middle range), and soil (long wavelengths). Research over the past decade has focused on developing methods and algorithms for soil moisture measurement. Much of the research was conducted in rangelands at the ARS Walnut Gulch Experimental Watershed in Arizona (Jackson *et al.*, 1993; Moran *et al.*, 1993; Schmugge *et al.*, 1993) and the ARS Little Washita River Watershed in Oklahoma (Jackson *et al.*, 1995; Jackson *et al.*, 1999; Starks and Jackson, 2002). Plate 6 shows a sequence of the changes in soil moisture over the 1997 Southern Great Plains Experiment (SGP '97).

Over the next five years, satellite microwave remote sensing will enter an era of vastly improved capabilities that will make it a more attractive source of information for rangeland applications. This era will begin with the launch of the Advanced Microwave Scanning Radiometer (AMSR) onboard NASA's Aqua satellite, followed by the European Space Agency's Envisat Advanced Synthetic Aperture Radar. NASA's Aqua satellite has an afternoon overpass, so Japan will soon launch a second AMSR onboard the ADEOS-II satellite with a morning overpass. Canada and Japan are planning to have additional satellite-borne microwave sensors in orbit in the next five years.

Thermal Infrared Imagery for Moisture Fluxes

With the launch of the Advanced Spaceborne Thermal Emission and Reflection radiometer (ASTER) on NASA's Terra satellite in December 1999, a new tool for studying the land surface from space became available (Yamaguchi *et al.*, 1998). This tool provides multispectral thermal infrared data; the airborne equivalent is the Thermal Infrared Multispectral Scanner (TIMS) which has six thermal infrared channels between 7 and 13 μm, as seen in Figure 11. These data can be used to estimate the spectral variation of the surface emissivity. The Temperature Emissivity Separation (TES) algorithm (Gillespie *et al.*, 1998) is used to extract the temperature and emissivities from either the TIMS or the ASTER data. The TES algorithm makes use of an empirical relation between the range of observed emissivities and their minimum value. The spectral emissivity data can be used as an additional tool to distinguish bare soil from vegetation, especially dry vegetation which has a similar spectral response to some soils in the visible and near-infrared portions of the spectrum. Because of their SiO_2 content, bare soils have a particularly strong emissivity feature between 8 and 9.5 μm, which is not present in the emissivity spectrum of vegetation. This feature was used by scientists with the Hydrology and Remote Sensing Laboratory (Beltsville, Maryland) to distinguish bare soil from senescent vegetation in their study of the El Reno area during the Southern Great Plains experiments in 1997 (French *et al.*, 2000) and in JORNEX (Schmugge *et al.*, 2002).

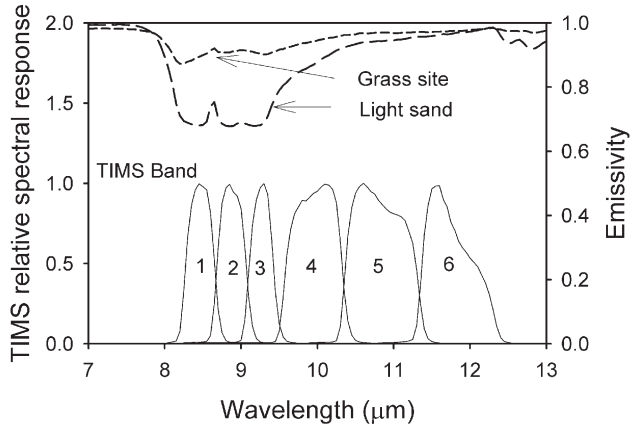

Figure 11. Relative spectral response of the Thermal Infrared Multispectral Scanner (TIMS) and the emissivities of a grass site and a light sandy site at the ARS Jornada Experimental Range. The emissivity data were obtained in September as the sites were drying during JORNEX.

Combining Visible and Infrared Imagery for Plant Water Assessment

The combination of visible and infrared measurements made with Landsat TM and ETM+ is a powerful source of information for temporal studies of natural resources. Scientists at the ARS Southwest Watershed Research Center derived a Water Deficit Index (WDI) from Landsat visible, near-infrared, and thermal-infrared imagery to detect temporal and spatial changes in grassland transpiration (Holifield *et al.*, in press). The WDI, which estimates relative evapotranspiration rates based on meteorological data and the relation between surface reflectance and temperature, has been successfully applied over heterogeneous terrain with little *a priori* information (Moran *et al.*, 1996). For the ARS Walnut Gulch Experimental Watershed during the summer monsoon period, the WDI was sensitive to both temporal and spatial changes in plant transpiration, as well as differences in transpiration caused by topography. The WDI was compared with a measure of plant available soil moisture (the Antecedent Retention Index, ARI), which was derived from an hourly record of precipitation and runoff, obtained from rain gauges and flumes located in the watershed. Results showed that there was a non-linear relation between the WDI and ARI, and implied that the WDI was the more sensitive indicator of vegetation health. Ultimately, the WDI approach may be used as a viable tool to monitor grassland health over heterogeneous regions.

Merging Imagery and other Geospatial Data

In most applications, remotely sensed imagery must be merged with other images or geospatial data within a GIS. Images and geospatial data have different map scales, orientations, pixel sizes, and other differences that make merging different data problematic. A good example is from the work of Peleg and Anderson (2002) shown in Figure 12. When two datasets are simply registered and resampled, with the same datum and map projection, the images can visually appear to be similar (Figures 12a and 12d). However, a scatterplot of the values for the different pixels from the first image with the value of the same pixel from the second image shows poor correlation (Figure 12c).

Because both images (Figures 12a and 12d) were acquired over the same experimental field, the two images should be the same; Peleg and Anderson (2002) developed a series of preprocessing steps for comparing images from

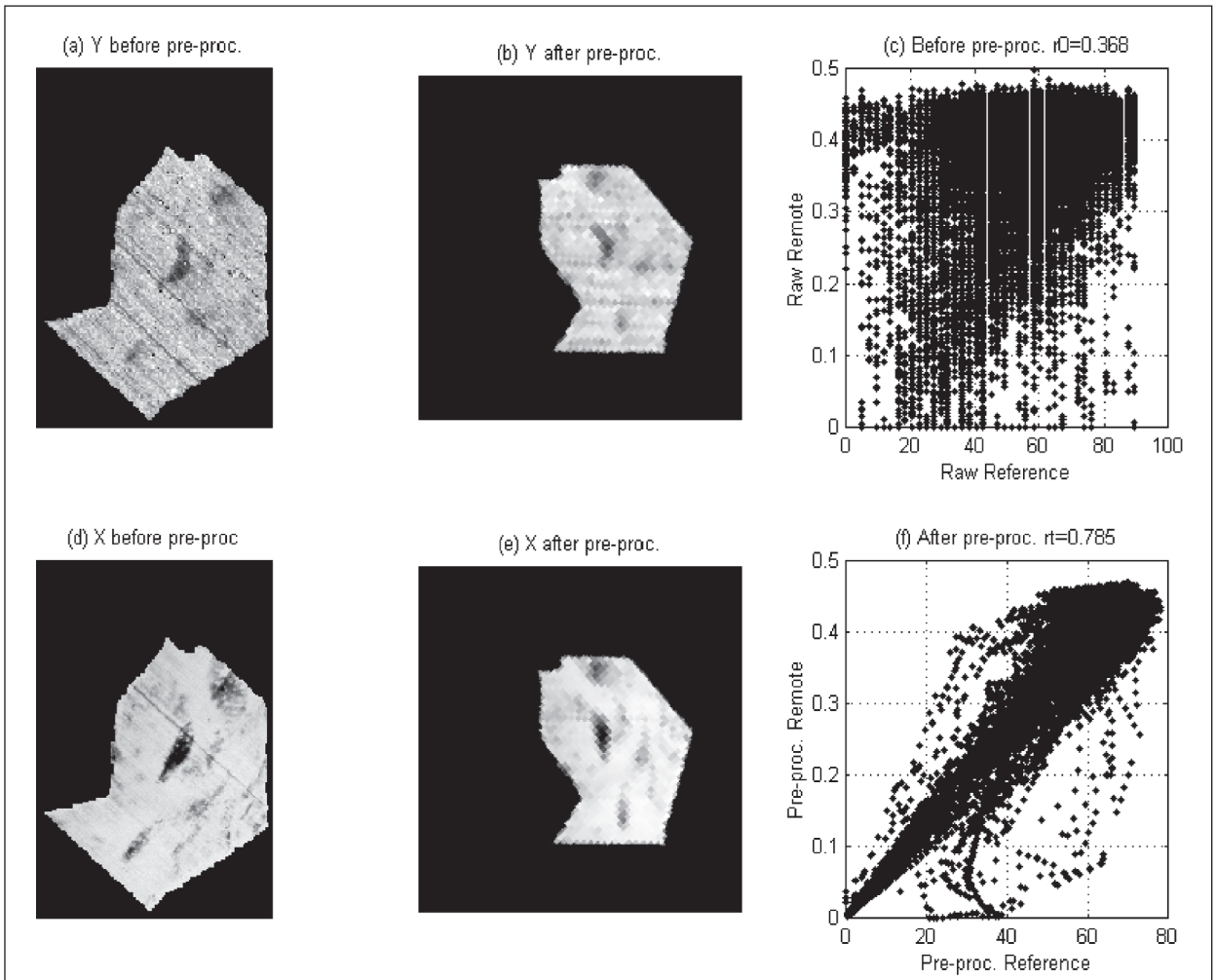

Figure 12. (a) Image **Y** before preprocessing and (b) image **Y** after preprocessing. (d) Image **X** before preprocessing and (e) image **X** after preprocessing. (c) The scatterplot between **Y** and **X** before preprocessing (r = 0.368) and (f) the scatterplot between **Y** and **X** after preprocessing (r = 0.785). Image **Y** was created from yield monitor data and image **X** is an NDVI image from airborne videography. These techniques are applicable to any situation where two images are required to be merged.

different sources. The preprocessing steps employ advanced mathematical procedures: a wavelet based transform, a pixel block transform, and an image rotation transform. These transforms were applied to the data to reduce sensor-specific noise to obtain Figures 12b and 12e. The scatterplot of pixel values from 12b and 12e show a much stronger correlation (Figure 12f). Pelleg and Anderson (2002) performed additional steps using Fast-Fourier-Transformation regression which reduced the amount of noise, and increased the correlation coefficient between the two images from 0.785 (in Figure 12f) to 0.963 (data not shown).

This example shows that low, simple correlations between the two images result from spatial errors, which occur even with small pixel sizes. Applications to rangeland management will require many different data sets merged within a GIS, each with its own amount of spatial error. With the advances in computing power that occur each year, it is feasible that these advanced algorithms will be incorporated into image processing software similar to the manner in which atmospheric, geometric, and radiometric algorithms are implemented today. In all likelihood, individual managers will be isolated from these processing steps, but will rely on the outputs, in much the same manner as people rely on weather reports from the National Weather Service without understanding the increasingly sophisticated algorithms used for weather prediction. And like the weather reports, there will be errors in determining rangeland health from remote sensing, but the size of the errors will be diminished with the increasing power and robustness of the analytical tools being developed.

Conclusions

Some techniques of remote sensing can be operational for rangeland health assessments, because first, the sensors are available, and second, the algorithms are well tested. These algorithms were not just developed by ARS scientists, even though the focus of this review was on the contribution by the ARS. Operational techniques are the use of large scale photographs and videography for noxious weeds, and soil and plant cover, and the use of Landsat, AVHRR, and MODIS for rangeland productivity. The user communities associated with these sensors will help ensure that similar data will continue to be available in the future.

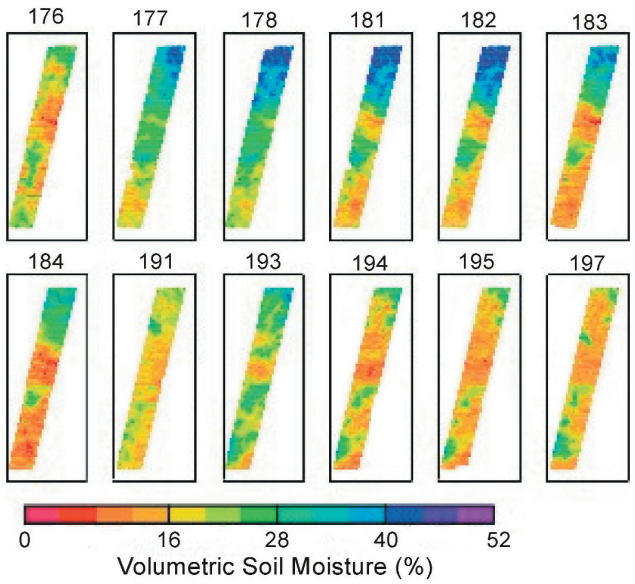

Plate 6. Maps of soil volumetric water content from the Electronically Scanned Thinned Array Radiometer (ESTAR), an airborne passive microwave sensor, for different year days of 1997. The ESTAR data were collected during the Southern Great Plains Experiment '97, the upper part of each image is the Kansas-Oklahoma border and the lower part of each image is the ARS Little Washita River Watershed.

Lidar and hyperspectral sensors are experimental. There is considerable scientific support for these sensors, and the results show how direct indicators of rangeland health can be remotely sensed. However, there is a considerable jump from experimental to operational satellites, due to the costs of launching satellites and maintaining data facilities. The costs are not cheap, but the extent of rangelands in the United States is large so that the cost per area is low compared to other methods. The economic benefits of healthy rangelands are difficult to quantify with reasonable accuracy.

Thermal and microwave sensors are much farther along the continuum from experimental to operational, in part because the economic impact of meteorological forecasts emphasizes the benefits in relation to the costs. Maintenance of hydrological functioning is another large class of rangeland ecosystem health indicators. The problem is that thermal and microwave data are not yet useful for direct indicators of ecosystem health. It will take more research to develop useful tools for assessment and monitoring with these sensors.

Remote sensing can measure the whole spatial extent, not just sample individual plots and assume these plots are representative. Every allotment has some areas that are better and some areas that are worse, so that the statistical errors from sampling individual plots can be large. Remotely sensed imagery, therefore, provides a balanced and fair approach to rangeland management. However, the adoption of remote sensing for rangeland management will depend on the widespread adoption of the ecosystem health paradigm. Even remote sensing techniques that "can be operational," will not be used if assessment and monitoring is based on rangeland "condition," determined from plant community succession.

Acknowledgments

This paper was written as a result of the ARS Remote Sensing Workshop, 13-15 November 2000, in Kansas City, Missouri. We thank Tom Schmugge, Tom Jackson, and Andy French for discussions.

References

Aase, J.K., A.B. Frank, and R.J. Lorenz, 1987. Radiometric reflectance measurements of northern Great Plains rangeland and crested wheatgrass pastures, *Journal of Range Management*, 40:299–302.

Anderson, G.L., J.H. Everitt, A.J. Richardson, and D.E. Escobar, 1993a. Using satellite data to map false broomweed (*Ericameria austrotexana*) infestations on south Texas rangelands, *Weed Technology*, 7:865–871.

Anderson, G.L., J.D. Hanson, and R.H. Haas, 1993b. Evaluating Landsat Thematic Mapper derived vegetation indices for estimating above-ground biomass on semiarid rangelands, *Remote Sensing of Environment*, 45:165–175.

Anderson, G.L., J.H. Everitt, D.E. Escobar, N.R. Spencer, and R.J. Andrascik, 1996. Mapping leafy spurge (*Euphorbia esula*) infestations using aerial photography and geographic information systems, *Geocarto International*, 11(1):81–89.

Anderson, G.L., C.W. Prosser, S. Haggar, and B. Foster, 1999. Change detection of leafy spurge infestations using aerial photography and geographic information systems, *Proceedings of the 17th Biennial Workshop Color Aerial Photography and Videography in Resource Assessment* (P. T. Tueller, editor), 05–07 May, Reno, Nevada, (American Society for Photogrammetry and Remote Sensing, Bethesda, Maryland), pp. 223–230.

Anderson, G.L., E.S. Delfosse, N.R. Spencer, C.W. Prosser, and R.D. Richard, 2003. Lessons in developing successive invasive weed control program, *Journal of Range Management*, 56:2–12.

Asrar, G., M. Fuchs, E.T. Kanemasu, and J.L. Hatfield, 1984. Estimating absorbed photosynthetically active radiation and leaf area index from spectral reflectance in wheat, *Agronomy Journal*, 76:300–306.

Briske, D.D., and R.K. Heitschmidt, 1991. An ecological perspective, *Grazing Management, An Ecological Perspective* (R.K. Heitschmidt and J.W. Stuth, editors), Timber Press, Portland, Oregon, pp. 11–26.

Carneggie, D.M., B.J. Schrumpf, and D.M. Mouat, 1983. Rangeland applications*, Manual of Remote Sensing Second Edition, Volume II* (R.N. Colwell, editor), American Society of Photogrammetry, Falls Church, Virginia, pp. 2325–2364.

Clark, P.E., M.S. Seyfried, and B. Harris, 2001. Intermountain plant community classification using Landsat TM and SPOT HRV data, *Journal of Range Management*, 54:152–160.

Clements, F.E., 1916. *Plant Succession: An Analysis of the Development of Vegetation*, Publication 242, Carnegie Institute of Washington, Washington, D.C., 512 p.

Curran, P.J., 1983. Multispectral remote sensing for the estimation of green leaf area index, *Philosophical Transactions of the Royal Society of London, Series A*, 309:257–270.

Daughtry, C.S.T., 2001. Discriminating crop residues from soil by shortwave infrared reflectance, *Agronomy Journal*, 93:125–131.

Daughtry, C.S.T., E.R. Hunt, Jr., C.L. Walthall, T.J. Gish, S. Liang, and E.J. Kramer, 2001. Assessing the spatial distribution of plant litter, *Proceedings of the Tenth JPL Airborne Earth Science Workshop* (R.O. Green, editor), 27 February–02 March, Pasadena, California (JPL Publication 02–1, Jet Propulsion Laboratory, National Aeronautics and Space Administration, Pasadena, California), pp. 105–114.

Dewey, S.A., K.P. Price, and D. Ramsey, 1991. Satellite remote sensing of Dyer's woad *(Isatis tinctoria*), *Weed Technology*, 5:479–484.

Driscoll, R.S., J.H. Everitt, R. Haas, and P.T. Tueller, 1997. Ranges and range management, *Manual of Photographic Interpretation* (W.R. Philipson, editor), American Society for Photogrammetry and Remote Sensing, Bethesda, Maryland, pp. 441–474.

Dyksterhuis, E.J., 1949. Condition and management of range land based on quantitative ecology, *Journal of Range Management*, 2:104–115.

Eidenshink, J.C., 1992. The 1990 Conterminous U. S. AVHRR data set, *Photogrammetric Engineering & Remote Sensing*, 58:809–813.

Eidenshink, J.E., and J.L. Fuandeen, 1994. The 1-km AVHRR global land data set: first stages in implementation, *International Journal of Remote Sensing*, 15:3443–3462.

Everitt, J.H., 1985. Using aerial photography for detecting blackbrush (*Acacia rigidula*) on south Texas rangelands, *Journal of Range Management*, 38:228–231.

Everitt, J.H., S.J. Ingle, H.W. Gausman, and H.S. Mayeux, Jr., 1984. Detection of false broomweed (*Ericameria austrotexana*) by aerial photography, *Weed Science*, 32:621–624.

Everitt, J.H., M.A. Hussey, D.E. Escobar, P.R. Nixon, and B. Pinkerton, 1986. Assessment of grassland phytomass with airborne video imagery, *Remote Sensing of Environment*, 20:299–306.

Everitt, J.H., R.D. Pettit, and M.A. Alaniz, 1987. Remote sensing of broom snakeweed (*Gutierrezia sarothrae*) and spiny aster (*Aster spinosus*), *Weed Science*, 35:295–302.

Everitt, J.H., and R. Villarreal, 1987. Detecting huisache (*Acacia farnesiana*) and Mexican palo-verde (*Parkinsonia aculeata*) by aerial photography, *Weed Science*, 35:427–432.

Everitt, J.H., D.E. Escobar, and A.J. Richardson, 1989. Estimating grassland phytomass production with near-infrared and mid-infrared spectral variables, *Remote Sensing of Environment*, 30:257–261.

Everitt, J.H., M.A. Alaniz, D.E. Escobar, and M.R. Davis, 1992. Using remote sensing to distinguish common (*Isocoma coronopifolia*) and Drummond goldenweed *(Isocoma drummondii*), *Weed Science*, 40:621–628.

Everitt, J.H., D.E. Escobar, R. Villarreal, M.A. Alaniz, and M.R. Davis, 1993a. Canopy light reflectance and remote sensing of shin oak (*Quercus havardii*) and associated vegetation, *Weed Science*, 41:291–297.

———, 1993b. Integration of airborne video, global positioning system, and geographic information system technologies for detecting and mapping two woody legumes on rangelands, *Weed Technology*, 7:981–987.

Everitt, J.H., J.V. Richerson, M.A. Alaniz, D.E. Escobar, R. Villarreal, and M.R. Davis, 1994. Light reflectance characteristics and remote sensing of Big Bend loco *(Astragalus mollissimus* var. *earlei*) and Wooton loco (*Astragalus wootonii*), *Weed Science*, 42:115–122.

Everitt, J.H., G.L. Anderson, D.E. Escobar, M.R. Davis, N.R. Spencer, and R.J. Andrascik, 1995a. Using remote sensing for detecting and mapping leafy spurge (*Euphorbia esula*), *Weed Technology*, 9:599–609.

Everitt, J.H., D.E. Escobar, and M.R. Davis, 1995b. Using remote sensing for detecting and mapping noxious plants, *Weed Abstracts*, 44:639–649.

Everitt, J.H., D.E. Escobar, M.A. Alaniz, M.R. Davis, and J.V. Richerson, 1996. Using spatial information technologies to map Chinese tamarisk, *Weed Science*, 44:194–201.

Everitt, J.H., D.E. Escobar, and M.R. Davis, 2001a. Reflectance and image characteristics of selected noxious rangeland species, *Journal of Range Management*, 54(suppl):A106–A120.

Everitt, J.H., C. Yang, B.J. Racher, C.M. Briton, and M.R. Davis, 2001b. Remote sensing of redberry juniper in the Texas Rolling Plains, *Journal of Range Management*, 54:254–259.

Ezra, C.E., L.R. Tinney, and R.D. Jackson, 1984. Effect of soil background on vegetation discrimination using Landsat data, *Remote Sensing of Environment*, 16:233–242.

Follett, R.F., J.M. Kimble, and R. Lal (editors), 2001. *The Potential of U.S. Grazing Lands to Sequester Carbon and Mitigate the Greenhouse Effect*, Lewis Publishers, Boca Raton, Florida, 442 p.

Frank, A.B., and J.K. Aase, 1994. Residue effects on radiometric reflectance measurements of northern Great Plains rangelands, *Remote Sensing of Environment*, 49:195–199.

French, A.N., T.J. Schmugge, and W.P. Kustas, 2000. Discrimination of senescent vegetation using thermal emissivity contrast, *Remote Sensing of Environment*, 74(2):249–254.

Friedel, M.H., 1991. Range condition assessment and the concept of thresholds: A viewpoint, *Journal of Range Management*, 44:422–426.

Gates, D.M., H.J. Keegan, J.C. Schleter, and V.R. Weidner, 1965. Spectral properties of plants, *Applied Optics*, 4:11–20.

Gausman, H.W., J.H. Everitt, A.H. Gerbermann, and R.L. Bowen, 1977a. Canopy reflectance and film image relations among three south Texas rangeland plants, *Journal of Range Management*, 30:449–450.

Gausman, H.W., R.M. Menges, D.E. Escobar, J.H. Everitt, and R.L. Bowen, 1977b. Pubescence affects spectra and imagery of silverleaf sunflower (*Helianthus argophyllus*), *Weed Science*, 25:437–440.

Gillespie, A.S. Rokugawa, T. Matsunaga, J.S. Cothern, S. Hook, and A.B. Kahle, 1998. A temperature and emissivity separation algorithm for Advanced Spaceborne Thermal Emission and Reflection Radiometer (ASTER) images, *IEEE Transactions on Geoscience and Remote Sensing*, 36:1113–1126.

Goetz, S.J., and S.D. Prince, 1999. Modelling terrestrial carbon exchange and storage: Evidence and implications of functional convergence in light-use efficiency, *Advances in Ecological Research*, 28:57–92.

Goodrich, D.C., A. Chehbouni, B. Goff, B. MacNish, T. Maddock, S. Moran, and 63 additional authors, 2000. Preface paper to the semi-arid land-surface-atmosphere (SALSA) program special issue, *Agricultural and Forest Meteorology*, 105:3–20.

Goward, S.N., and K.F. Huemmrich, 1992. Vegetation canopy IPAR absorptance and the normalized difference vegetation index: An assessment using the SAIL model, *Remote Sensing of Environment*, 39:119–140.

Gower, S.T., C.J. Kucharik, and J.M. Norman, 1999. Direct and indirect estimation of leaf area index, f_{apar}, and net primary production of terrestrial ecosystems, *Remote Sensing of Environment*, 70:29–51.

Green, R.O., M.L. Eastwood, and O. Williams, 1998. Imaging Spectroscopy and the Airborne Visible Infrared Imaging Spectrometer (AVIRIS), *Remote Sensing of Environment*, 65:227–248.

Hatfield, J.L., G. Asrar, and E.T. Kanemasu, 1984. Intercepted photosynthetically active radiation estimated by spectral reflectance, *Remote Sensing of Environment*, 14:65–75.

Hatfield, J.L., E.T. Kanemasu, G. Asrar, R.D. Jackson, P.J. Pinter, Jr., R.J. Reginato, and S.B. Idso, 1985. Leaf-area estimates from spectral measurements over various planting dates of wheat, *International Journal of Remote Sensing*, 6:167–175.

Havstad, K.M., W.P. Kustas, A. Rango, J.C. Ritchie, and T.J. Schmugge, 2000. Jornada Experimental Range: A unique arid land location for experiments to validate satellite systems and to understand effects of climate change, *Remote Sensing of Environment*, 74:13–25.

Holecheck, J.L., 1988. An approach for setting the stocking rate, *Rangelands*, 10(1):10–14.

Holifield, C.D., S. McElroy, M.S. Moran, R. Bryant, and T. Miura, in press. Temporal and spatial changes in grassland transpiration detected using Landsat TM and ETM+ Imagery, *Canadian Journal of Remote Sensing*.

Huete, A.R., 1988. A soil-adjusted vegetation index (SAVI), *Remote Sensing of Environment*, 25:295–309.

Huete, A.R., R.D. Jackson, and D.F. Post, 1985. Spectral response of a plant canopy with different soil backgrounds, *Remote Sensing of Environment*, 17:37–53.

Hunt, E.R., Jr., 1994. Relationship between woody biomass and PAR conversion efficiency for estimating net primary production from NDVI, *International Journal of Remote Sensing*, 15:1725–1730.

———, 2003. Leaf area index and cover of shortgrass steppe using AVIRIS imagery, *Proceedings of the Eleventh JPL Airborne Earth Science Workshop* (R.O. Green, editor), 05-08 March 2002, Pasadena, California (Jet Propulsion Laboratory, National Aeronautics and Space Administration, Pasadena, California).

Hunt, E.R., Jr., and S.W. Running, 1992. Simulated dry matter yields for aspen and spruce stands in the North American boreal forest, *Canadian Journal of Remote Sensing*, 18:126–133.

Jackson, T.J., D.M. Le Vine, A.J. Griffis, D.C. Goodrich, T.J. Schmugge, C.T. Swift, and P.E. O'Neill, 1993. Soil moisture and rainfall estimation over a semiarid environment with the ESTAR microwave radiometer, *IEEE Transactions on Geoscience and Remote Sensing*, 31:836–841.

Jackson, T.J., D.M. Le Vine, C.T. Swift, T.J. Schmugge, and F.R. Schiebe, 1995. Large scale mapping of soil moisture using the ESTAR passive microwave radiometer in Washita '92, *Remote Sensing of Environment*, 53:27–37.

Jackson, T.J., D.M. Le Vine, A.Y. Hsu, A. Oldak, P.J. Starks, C.T. Swift, J.D. Isham, and M. Haken, 1999. Soil moisture mapping at regional scales: The Southern Great Plains Hydrology Experiment, *IEEE Transactions on Geoscience and Remote Sensing*, 37:2136–2151.

James, L.F., R.F. Keeler, A.E. Johnson, M.C. Williams, E.M. Cronin, and J.D. Olsen, 1980. *Plants Poisonous to Livestock in the Western United States*, Agricultural Information Bulletin 415, U.S. Department of Agriculture, Washington, D.C., 90 p.

Kiniry, J.R., C.R. Tischler, and G.A. Van Esbroeck, 1999. Radiation use efficiency and leaf CO_2 exchange for diverse C_4 grasses, *Biomass and Bioenergy*, 17:95–112.

King, D., 1995. Airborne multispectral digital camera and video sensors, *Canadian Journal of Remote Sensing*, 21:245–273.

Knipling, E.B., 1970. Physical and physiological basis for the reflectance of visible and near-infrared radiation from vegetation, *Remote Sensing of Environment*, 1:155–159.

Kokaly, R.F., R.R. Root, K. Brown, G.L. Anderson, and S. Hager, in press. Calibration of Compact Airborne Spectrographic Imager (CASI) data to surface reflectance at Theodore Roosevelt National Park for mapping invasive species, *International Journal of Remote Sensing*.

Krabill, W.B., J.G. Collins, L.E. Link, R.N. Swift, and M.L. Butler, 1984. Airborne laser topographic mapping results, *Photogrammetry Engineering & Remote Sensing*, 50:685–694.

Kumar, M., and J.L. Monteith, 1981. Remote sensing of crop growth, *Plants and the Daylight Spectrum* (H. Smith, editor), Academic Press, London, United Kingdom, pp. 133–144.

Kustas, W.P., and D.C. Goodrich, 1994. Preface MONSOON '90 Multidisciplinary Experiment, *Water Resources Research*, 30:1211–1225.

Landsberg, J.J., and R.H. Waring, 1997. A generalised model of forest productivity using simplified concepts of radiation-use efficiency, carbon balance and partitioning, *Forest Ecology and Management*, 95:209–228.

Lass, L.W., and R.H. Callihan, 1997. The effect of phenological stage on detectability of yellow hawkweed (*Heiracium pratense*) and oxeye daisy (*Chrysanthemum leucanthemum*) with remote multispectral digital imagery, *Weed Technology*, 11:248–256.

Lass, L.W., H.W. Carson, and R.H. Callihan, 1996. Detection of yellow starthistle (*Centaurea solstitialis*) and common St. Johnswort (*Hypericum perforatum*) with multispectral digital imagery, *Weed Technology*, 10:466–474.

Laycock, W.A., 1991. Stable states and thresholds of range condition on North American rangelands: A viewpoint, *Journal of Range Management*, 44:427–433.

Liu, W.T., and F.N. Kogan, 1996. Monitoring regional drought using the Vegetation Condition Index, *International Journal of Remote Sensing*, 17:2761–2782.

Mausel, P.W. (editor), 1995. *Proceedings 15th Biennial Workshop on Videography and Color Photography in Resource Assessment*, 01–03 May, Terre Haute, Indiana (American Society of Photogrammetry and Remote Sensing, Bethesda, Maryland), 372 p.

Mayeux, H.S., Jr., and C.J. Scifres, 1978. Goldenweeds-New perennial range weed problems, *Rangelands*, 5:91–93.

———, 1981. Drummond's goldenweed and its control with herbicides, *Journal of Range Management*, 34:98–101.

McGwire, K., T. Minor, and L. Fenstermaker, 2000. Hyperspectral mixture modeling for quantifying sparse vegetation cover in arid environments, *Remote Sensing of Environment*, 72:360–374.

Menenti, M., and J.C. Ritchie, 1994. Estimation of effective aerodynamic roughness of Walnut Gulch watershed with laser altimeter measurements, *Water Resources Research*, 30(5):1329–1337.

Millington, A.C., J. Wellens, J.J. Settle, and R.J. Saull, 1994. Explaining and monitoring land cover dynamics in drylands using multitemporal analysis of NOAA AVHRR imagery, *Environmental Remote Sensing from Regional to Global Scales* (G. Foody and P. Curran, editors), John Wiley & Sons, Chichester, United Kingdom, pp. 16–43.

Monteith, J.L., 1977. Climate and the efficiency of crop production in Britain, *Philosophical Transactions of the Royal Society of London, Series B*, 281:277–294.

Moran, M.S., D.C. Hymer, J. Qi, and E.E. Sano, 1993. Soil moisture evaluation using Synthetic Aperture Radar (SAR) and optical remote sensing in semiarid rangeland, *Agricultural and Forest Meteorology*, 105:69–80.

Moran, M.S., T.R. Clarke, W.P. Kustas, M. Weltz, S.A. Amer, and A.R. Huete, 1994. Evaluation of hydrologic parameters in semi-arid rangeland using remotely sensed spectral data, *Water Resources Research*, 30:1287–1297.

Moran, M.S., A.F. Rahman, J.C. Washburne, D.C. Goodrich, M.A. Weltz, and W.P. Kustas, 1996. Combining the Penman-Monteith equation with measurements of surface temperature and reflectance to map regional evaporation rates, *Agricultural and Forest Meteorology*, 80:87–109.

Myneni, R.B., and D.L. Williams, 1994. On the relationship between FAPAR and NDVI, *Remote Sensing of Environment*, 49:200–211.

Nouvellon, Y., D. Lo Seen, S. Rambal, A. Bégué, M.S. Moran, Y. Kerr, and J. Qi, 2000. Time course of radiation use efficiency in a shortgrass ecosystem: Consequences for remotely sensed estimation of primary production, *Remote Sensing of Environment*, 71:43–55.

Nouvellon, Y., M.S. Moran, D. Lo Seen, R. Bryant, S. Rambal, W. Ni, A. Bégué, A. Chehbouni, W.E. Emmerich, P. Heilman, and J. Qi, 2001. Coupling a grassland ecosystem model with Landsat imagery for a 10-year simulation of carbon and water budgets, *Remote Sensing of Environment*, 78:131–149.

NRC, 1994. *Rangeland Health, New Methods to Classify, Inventory and Monitor Rangelands*, National Research Council, National Academy Press, Washington, D.C., 180 p.

NRCS, 1994. *National Resources Inventory Highlights*, Natural Resources Conservation Service, United States Department of Agriculture, Washington, D.C., 4 p.

———, 1997. *National Range and Pasture Handbook*, Grazing Lands Technology Institute, Natural Resource Conservation Service, United States Department of Agriculture, Washington, D.C., 448 p.

Pachepsky, Y.A., J.C. Ritchie, and D. Gimenez, 1997. Fractal modeling of airborne laser altimetry data, *Remote Sensing of Environment*, 61:150–161.

Pachepsky, Y.A., and J.C. Ritchie, 1998. Seasonal changes in fractal landscape surface roughness estimated from airborne laser altimetry data, *International Journal of Remote Sensing*, 19(13):2509–2516.

Parker Williams, A., and E.R. Hunt, Jr., 2002. Estimation of leafy spurge cover from hyperspectral imagery using mixture-tuned matched filtering, *Remote Sensing of Environment*, 82:446–456.

Peleg, K., and G.L. Anderson, 2002. FFT regression and cross-noise reduction for comparing images in remote sensing, *International Journal of Remote Sensing*, 23:2097–2124.

Pellant, M., P. Shaver, and K. Spaeth, 1999. Field test of a prototype rangeland inventory procedure in the western USA, *Proceedings of the VI International Rangeland Congress, People and Rangelands, Building the Future, Volume 2* (D. Eldridge and D. Freudenberger, editors), 19-23 July, Townsville, Australia (VI International Rangeland Congress, Aitkenvale, Queensland, Australia), pp. 766–767.

Pellant, M., P. Shaver, D.A. Pyke, and J.E. Herrick, 2000. *Interpreting Indicators of Rangeland Health (Version 3)*, Technical Reference 1734-6, National Science and Technology Center, Bureau of Land Management, United States Department of Interior, Denver, Colorado, 130 p.

Price, J.C., 1993. Estimating leaf area index from satellite data, *IEEE Transactions on Geoscience and Remote Sensing*, 31:727–734.

Price, J.C., and W.C. Bausch, 1995. Leaf area index estimation from visible and near-infrared reflectance data, *Remote Sensing of Environment*, 52:55–65.

Prince, S.D., 1991. A model of regional primary production for use with coarse resolution satellite data, *International Journal of Remote Sensing*, 12:1313–1330.

Prince, S.D., and S.N. Goward, 1995. Global primary production: a remote sensing approach, *Journal of Biogeography*, 22:815-835.

Qi, J., A. Chehbouni, A.R. Huete, Y.H. Kerr, and S. Sorooshian, 1994. A modified soil adjusted vegetation index, *Remote Sensing of Environment*, 48:119–126.

Qi, J., R.C. Marsett, and P. Heilman, 2000a. Rangeland vegetation cover estimation from remotely sensed data, *Proceedings of the Second International Conference on Geospatial Information in Agriculture and Forestry*, 10–12 January, Lake Buena Vista, Florida (ERIM International, Ann Arbor, Michigan), 2:243–252.

Qi, J., R.C. Marsett, M.S. Moran, D.C. Goodrich, P. Heilman, Y.H. Kerr, G. Dedieu, A. Chehbouni, and X.X. Zhang, 2000b. Spatial and temporal dynamics of vegetation in the San Pedro River Basin Area, *Agricultural and Forest Meteorology*, 105:55–68.

Qi, J., Y.H. Kerr, M.S. Moran, M. Weltz, A.R. Huete, S. Sorooshian, and R. Bryant, 2000c. Leaf area index estimates using remotely sensed data and BRDF models in a semiarid region, *Remote Sensing of Environment*, 73:18–30.

Quimby, P.C., Jr., and L. Wendel, 1997. *The Ecological Area-Wide Management (TEAM) - Leafy Spurge*, USDA Agricultural Research Service, Sidney, Montana, 51 p.

Rango, A., J.C. Ritchie, W.P. Kustas, T.J. Schmugge, K.S. Humes, L.E. Hipps, J.H. Prueger, and K.M. Havstad, 1998. JORNEX: A multidisciplinary remote sensing campaign to quantify plant community/atmospheric interactions in the northern Chihuahuan desert of New Mexico, *Hydrology in a Changing Environment* (H. Wheater and C. Kirby, editors), John Wiley, London, United Kingdom, pp. 585–590.

Rango, A., M.J. Chopping, J.C. Ritchie, K.M. Havstad, W.P. Kustas, and T.J. Schmugge, 2000. Morphological characteristics of shrub-coppice dunes in desert grasslands of southern New Mexico derived from scanning lidar, *Remote Sensing of Environment*, 74:26–44.

Rees, N.E., and N.R. Spencer, 1991. Biological control of leafy spurge, *Noxious Range Weeds*, (L.F. James, J.O. Evans, M.H. Ralphs, and R.D. Child, editors), Westview Press, Boulder, Colorado, pp. 182–192.

Reeves, M.C., J.C. Winslow, and S.W. Running, 2001. Mapping weekly rangeland vegetation productivity, *Journal of Range Management*, 54(suppl):A90–A105.

Richardson, A.J., D.E. Escobar, H.W. Gausman, and J.H. Everitt, 1981. Use of Landsat-2 data technique to estimate silverleaf sunflower infestation, *Proceedings of Machine Processing of Remotely Sensed Data Symposium*, 23–26 June, Purdue University, West Lafayette, Indiana, pp. 676–683.

Richardson, A.J., J.H. Everitt, and H.W. Gausman, 1983. Radiometric estimation of biomass and nitrogen content of Alicia grass, *Remote Sensing of Environment*, 13:179–184.

Ritchie, J.C., J.H. Everitt, D.E. Escobar, T.J. Jackson, and M.R. Davis, 1992. Airborne laser measurements of rangeland canopy cover, *Journal of Range Management*, 45(2):189–193.

Ritchie, J.C., D.L. Evans, D.M., Jacobs, J.H. Everitt, and M.A. Weltz, 1993a. Measuring canopy structure with an airborne laser altimeter, *Transactions of the American Society of Agricultural Engineers*, 36(4):1235–1238.

Ritchie, J.C., T.J. Jackson, E.H. Grissinger, J.B. Murphey, J.D. Garbrecht, J.H. Everitt, D.E. Escobar, M.R. Davis, and M.A. Weltz, 1993b. Airborne altimeter measurements of landscape properties, *Hydrological Sciences Journal*, 38(3):403–416.

Ritchie, J.C., K.S. Humes, and M.A. Weltz, 1995. Laser altimeter measurements at Walnut Gulch Watershed, Arizona, *Journal of Soil and Water Conservation*, 50:440–442.

Ritchie, J.C., A. Rango, W.P. Kustas, T.J. Schmugge, K.M. Havstad, J.H. Everitt, L.E. Hipps, and K. Ramalingham, 1998. JORNEX: A remote sensing campaign to study plant community response to hydrologic fluxes in desert grasslands, *Rangeland Management and Water Resources* (D.F. Potts, editor), American Water Resources Society, Herndon, Virginia, pp. 65–74.

Ritchie, J.C., M.S. Seyfried, M.J. Chopping, and Y. Pachepsky, 2001. Airborne laser technology for measuring rangeland conditions, *Journal of Range Management*, 54(suppl):A8–A21.

Roberts, D.A., M. Gardner, R. Church, S. Ustin, G. Scheer, and R.O. Green, 1998. Mapping chaparral in the Santa Monica mountains using multiple endmember spectral models, *Remote Sensing of Environment*, 65:267–279.

Rouse, J.W., R.H. Haas, J.A. Schell, and D.W. Deering, 1974. Monitoring vegetation systems in the Great Plains with ERTS, *Third Earth Resources Technology Satellite–1 Symposium. Volume I: Technical Presentations* (S.C. Freden, E.P. Mercanti, M. Becker, editors), 10–14 December 1973, Washington, D.C. (NASA SP-351, National Aeronautics and Space Administration, Washington, D.C.), pp. 309–317.

Ruimy, A., G. Dedieu, and B. Saugier, 1994. Methodology for the estimation of terrestrial net primary production from remotely sensed data, *Journal of Geophysical Research*, 99:5263–5283.

Ruimy, A., P.G. Jarvis, D.D. Baldocchi, and B. Saugier, 1995. CO_2 fluxes over plant canopies and solar radiation: A review, *Advances of Ecological Research*, 26:1–66.

Running, S.W., and E.R. Hunt, Jr., 1993. Generalization of a forest ecosystem process model for other biomes, BIOME-BGC, and an application for global-scale models, *Scaling Physiological Processes: Leaf to Globe* (J.R. Ehleringer and C. Field, editors), Academic Press, San Diego, California, pp. 141–158.

Sampson, A.W., 1919. *Plant Succession Relation to Range Management*, USDA Technical Bulletin No. 791, United States Department of Agriculture, Washington, D.C., 76 p.

Schmugge, T.J., T.J. Jackson, W.P. Kustas, and J.R. Wang, 1992. Passive microwave remote sensing of soil moisture: Results from HAPEX, FIFE and MONSOON 90, *ISPRS Journal of Photogrammetry and Remote Sensing*, 47:127–143.

Schmugge, T., A. French, J.C. Ritchie, A. Rango, and H. Pelgrum, 2002. Temperature and emissivity separation from multispectral thermal infrared observations, *Remote Sensing of Environment*, 79:189–198.

Scifres, C.J., 1980. *Brush Management,* Texas A & M University Press, College Station, Texas, 360 p.

Sheley, R.L., and J.K. Petroff (editors), 1999. *Biology and Management of Noxious Rangeland Weeds*, Oregon State University Press, Corvallis, Oregon, 438 p.

Sinclair, T.R., and T. Horie, 1989. Leaf nitrogen, photosynthesis, and crop radiation use efficiency: A review, *Crop Science*, 29:90–98.

Sinclair, T.R., and R.C. Muchow, 1999. Radiation use efficiency, *Advances of Agronomy*, 65:215–265.

Spaeth, K.E., M. Pellant, and P. Shaver, 1999. Natural resource inventory on BLM lands in Colorado: An analysis of rangeland health, *Proceedings of the VI International Rangeland Congress, People and Rangelands, Building the Future* (D. Eldridge and D. Freudenberger, editors), 19-23 July, Townsville, Australia (VI International Rangeland Congress, Aitkenvale, Queensland, Australia), 2:801–802.

Sperry, O.E., J.W. Dollahite, G.O. Hoffman, and B.J. Camp, 1964. *Texas Plants Poisonous to Livestock*, Texas Agricultural Experiment Station Bulletin 1028, Texas A & M University, College Station, Texas, 59 p.

SRM (Society for Range Management Task Group on Unity in Concepts and Terminology Committee), 1995. New concepts for assessment of rangeland condition, *Journal of Range Management*, 48:271–282.

Starks, P.J., and T.J. Jackson, 2002. Estimating soil water content in tallgrass prairie using remote sensing, *Journal of Range Management*, 55:474–481.

Strong, L.L., R.W. Dana, and L.H. Carpenter, 1985. Estimating phytomass of sagebrush habitat types from microdensitometer data, *Photogrammetric Engineering & Remote Sensing*, 51:467–474.

Tucker, C.J., L.D. Miller, and R.L. Pearson, 1975. Shortgrass prairie spectral measurements, *Photogrammetric Engineering & Remote Sensing*, 41:1157–1162.

Tucker, C.J., C. Vanpraet, E. Boerwinkel, and A. Gaston, 1983. Satellite remote sensing of total dry matter production in the Senegalese sahel, *Remote Sensing of Environment*, 13:461–474.

Tueller, P.T., 1982. Remote sensing for range management, *Remote Sensing for Resource Management* (C.J. Johannsen and J.L. Sanders, editors), Soil Conservation Society of America, Ankeny, Iowa, pp. 125–140.

———, 1989. Remote sensing technology for rangeland management applications, *Journal of Range Management*, 42:442–453.

———, 1992. Overview of remote sensing for range management, *Geocarto International*, 1:5–10.

———, 1995. Remote sensing in the management of rangelands, *Annals of the Arid Zone*, 34:191–207.

Ustin, S.L., D. DiPietro, K. Olmstead, E. Underwood, and G. Scheer, 2002. Hyperspectral remote sensing for invasive species detection and mapping, *Proceedings of IGARSS 2002: International Geoscience and Remote Sensing Symposium*, 24-28 June, Toronto, Ontario, Canada (IEEE and the Canadian Society for Remote Sensing), 3:1658–1660.

Vitousek, P.M., C.M. D'Antonio, L.L. Loope, and R. Westbrooks, 1996. Biological invasions as global environmental change, *American Scientist*, 84:468–478.

Vogelmann, J.E., S.M. Howard, L. Yang, C.R. Larson, B.K. Wylie, and N. Van Driel, 2001. Completion of the 1990s National Land Cover Data Set for the conterminous United States from Landsat Thematic Mapper data and ancillary data sources, *Photogrammetric Engineering & Remote Sensing*, 67:650–662.

Washington-Allen, R.A., N.E. West, R.D. Ramsey, and C.T. Hunsaker, 1999. Characterization of the ecological integrity of commercially grazed rangelands using remote sensing-based ecological indicators, *Proceedings of the VI International Rangelands Congress: People and Rangelands, Building the Future* (D. Eldridge and D. Freudenberger, editors), 17-23 July, Townsville, Queensland, Australia (VI International Rangeland Congress, Aitkenvale, Queensland, Australia), 2:778–780.

Weltz, M.A., J.C. Ritchie, and H.D. Fox, 1994. Comparison of laser and field measurements of vegetation heights and canopy cover, *Water Resources Research*, 30(5):1311–1320.

West, N.E., and E.L. Smith, 1997. Improving the monitoring of rangelands, *Rangelands*, 19(6):9–14.

Winslow, J.C., E.R. Hunt, Jr., and S.C. Piper, 2001. Models of solar irradiance based on daily humidity, precipitation and temperature data for various spatial scales and global-change applications, *Ecological Modelling*, 143:227–243.

Yamaguchi, Y., A.B. Kahle, H. Tsu, T. Kawakami, and M. Pniel, 1998. Overview of Advanced Spaceborne Thermal Emission and Reflection Radiometer (ASTER), *IEEE Transactions on Geoscience and Remote Sensing*, 36:1062–1071.

Yang, L., B.K. Wylie, L.L. Tieszen, and B.C. Reed, 1998. An analysis of relationships among climate forcing and time-integrated NDVI of grasslands over the U.S. Northern and Central Great Plains, *Remote Sensing of Environment*, 65:25–37.

Yokoya, N., K. Yamamoto, and N. Funakuro, 1989. Fractal-based analysis and interpolation of 3D natural surface shapes and their application to terrain modeling, *Computer Vision, Graphics, and Image Processing*, 46:284–302.